



Master of Science in Physics
Specialisation in Subatomic Physics and Astroparticles

Academic year: **2023-2024**

Sacha REJAI

Phenomenology at the future FCCee detector sensitivity to exotic long-lived particles

Master 2 internship report
under the supervision of
Éric CONTE and **Ziad EL BITAR**

01 March 2024 to 28 June 2024



Contents

Abstract	i
Acknowledgments	ii
Abbreviations	iii
1 Introduction	1
1.1 Scientific context	1
1.2 Aims	1
1.3 Report outlines	1
2 Building the theoretical model of heavy neutrinos	2
2.1 Reminder of the electroweak Standard Model	2
2.1.1 The Noether procedure	3
2.1.2 The Higgs mechanism and particle masses	3
2.1.3 Interactions involving the neutrino	4
2.2 Extending the Standard Model with one generation of light and heavy neutrinos	4
2.2.1 Dirac and Majorana mass terms	4
2.2.2 Masses in in the framework of type-I Seesaw Model	5
2.2.3 Interactions in in the framework of type-I Seesaw Model	6
2.3 Generalization to three generations of leptons	7
2.4 Experimental constraints	7
3 Study of the heavy-neutrinos phenomenology at FCC-ee	8
3.1 Framework of the study	8
3.1.1 The FCC-ee	8
3.1.2 Simplified assumptions on the model	9
3.1.3 Techniques of calculation	9
3.1.4 Validation of the results	10
3.2 Indirect production of the heavy neutrinos	10
3.2.1 Decay width calculation	10
3.2.2 Chirality and helicity analysis	11
3.2.3 Limit on the heavy neutrino mass and mixing term	12
3.3 Direct production of the heavy neutrinos	14
3.4 Decay of the heavy neutrinos	16
3.5 Flight distance of the heavy neutrinos at FCC-ee	18

4	Signature of a long-lived heavy neutrino in the CLD detector	19
4.1	Signal and background sources	19
4.2	Production of Monte-Carlo samples	19
4.3	The CLD detector and detector simulation	19
4.4	Parametrisation of the reconstructed tracks	20
4.5	Influence of the model parameters on the reconstructed tracks	21
5	Conclusion	22
	Bibliography	22
	Appendix A : SM and HNL's Feynman Rules	25
	Appendix B : Chirality and helicity projectors	27
	Appendix C : Trace identities of Dirac matrices	29
	Appendix D : Full computation of decay-width and cross-sections	30
	Appendix E : Cards for generation and simulation	47

Résumé

Les leptons neutres lourds (dits HNL pour Heavy Neutral Leptons) sont des particules hypothétiques qui correspondraient à des neutrinos plus lourds que ceux actuellement connus et de chiralité droite. Leur existence permettrait de construire un terme de masse pour les neutrinos légers (terme absent dans le Modèle Standard) et ils pourraient constituer des candidats à la matière noire. Le stage est dédié à la phénoménologie d'une extension du Modèle Standard dans lequel la masse des neutrinos est obtenue par un mécanisme SeeSaw de type 1. Les interactions possibles entre les neutrinos lourds et les particules standards ont été dérivées. Nous nous sommes intéressés ensuite à la production au FCC (Future Circular Collider) de neutrinos lourds à long-temps de vie à l'issue des collisions e^+e^- d'une énergie de 91 GeV. A partir des calculs de section efficaces et de largeurs de désintégration, la région des paramètres correspondant à un long temps de vie pertinent pour les expérimentateurs a été identifiée. En utilisant les programmes MadGraph, Pythia et Delphes, la reconstruction par le détecteur CLD (CLIC-Like Detector) de traces issues des produits de désintégration des neutrinos lourds a été investiguée en regardant des observables telles que la multiplicité de traces ou le paramètre d'impact.

Mots-Clés : leptons neutres lourds; FCC-ee; mécanisme SeeSaw de type 1; particules à long-temps de vie

Abstract

Heavy Neutral Leptons (HNL) are hypothetical particles that would correspond to neutrinos heavier than those currently known, and of right-hand chirality. Their existence would make it possible to construct a mass term for light neutrinos (a term absent in the Standard Model), and they could be candidates for dark matter. The internship is dedicated to the phenomenology of an extension of the Standard Model in which neutrino mass is obtained by a SeeSaw type 1 mechanism. Possible interactions between heavy neutrinos and standard particles have been derived. We then turned our attention to the production at the FCC (Future Circular Collider) of long-lived heavy neutrinos from e^+e^- collisions with an energy of 91 GeV. Based on calculations of effective cross-sections and decay widths, the parameter region corresponding to a long lifetime relevant to experimentalists was identified. Using the MadGraph, Pythia and Delphes programs, the CLD (CLIC-Like Detector) reconstruction of traces from heavy neutrino decay products was investigated, looking at observables such as trace multiplicity and impact parameter.

Keywords: Heavy neutral leptons; FCC-ee; SeeSaw type 1 mechanism; long-lived particles

Acknowledgments

I would like to extend my deepest gratitude to all those who have supported and guided me throughout the duration of my internship at the IPHC laboratory.

First and foremost, I would like to thank my supervisors, Éric Conte and Ziad El Bitar, for their invaluable guidance, expertise, and encouragement. Their insights and advice have been instrumental in shaping my understanding and approach to the research conducted in the PICSEL group. Their patience and willingness to share their extensive knowledge have made this learning experience both enriching and enjoyable.

I am also grateful to the entire PICSEL group at IPHC for their collaborative spirit and the supportive environment they provided. The group's collective dedication to research and innovation has been inspiring, and I have greatly benefited from the numerous discussions and interactions with its members.

Additionally, I would like to express my sincere thanks to Auguste Besson, the leader of the PICSEL team, and Sandrine Courtin, the headmaster of IPHC, for their support and leadership.

Lastly, I would like to thank my colleagues and friends who have been part of this journey. Their support and camaraderie have made this experience memorable and fulfilling.

This internship has been a significant milestone in my academic and professional journey, and I am sincerely thankful to everyone who has contributed to its success.

Abbreviations

BSM	Beyond the Standard Model
CLD	CLIC-Like Detector
COM	Center Of Mass
EFT	Effective Field Theory
FCCee	Future Circular electron-positron Collider
HNL	Heavy Neutral Lepton
LH	Left handed
LLP	Long-Lived Particle
RH	Right handed
SM	Standard Model
SB	Symmetry Breaking
SSB	Spontaneous Symmetry Breaking
VEV	Vaccum Expectation Value

1 Introduction

This M2 internship will take place in the IPHC institute (Institut Pluridisciplinaire Hubert Curien) at Strasbourg, more precisely in the DRS department (Subatomic Research Department). The scientific expertise of the DRS explores fields as varied as nucleus physics, particle physics and astroparticle physics, as well as more applied fields, often at the frontier between disciplines, such as radiochemistry and radiation protection. The internship has been hosted in the PICSEL group (Physics with Integrated Cmos Sensors and ELection machines). This group develops active monolithic pixel sensors, mainly for trajectographs and vertex detectors for current and future particle physics experiments. It is also taking part in the FCC collaboration, for the development of future detectors.

1.1 Scientific context

Particle physics emerged in the 20th century. The state of our knowledge has continued to grow, with the discovery of all the elementary particles of the Standard Model, their properties and their interactions. The latest main discovery, the Higgs boson in 2012, validated the theoretical predictions that explained the mass of the particles. The Standard Model of particle physics provides predictions that are in perfect agreement with experimental results, but some questions remain.

One of these is neutrino mass. This particle was considered initially massless until the experimental observation of neutrino oscillation requires the opposite. This discovery led to two major problems. First, a mechanism had to be added to give neutrinos mass, which is forbidden in the Standard Model. Second, we have to explain why the mass is so small.

1.2 Aims

The main goal of the internship is to study an extension of the Standard Model where the problem of mass term for neutrinos is fixed and an explanation of the smallness of the mass is given. This theoretical model is the Seesaw model of type I. One phenomenological consequence of this model is the requirement of sterile neutrinos, also called heavy neutral leptons, which can be searched at hadronic or leptonic colliders.

The PICSEL group is very interested in this model because heavy neutrinos can be long-lived *i.e.* they can "flight" from centimeters to meters in the detectors before decaying. This property can lead to many promising and exotic signatures of new physics. In particular, reconstruction of displaced vertices or displaced tracks can take advantage of the group's expertise in tracker development.

1.3 Report outlines

The structure of this report is organized into three main sections, each addressing a specific aspect of the research.

In the first major section, we begin by revisiting the Electroweak Standard Model, covering foundational concepts such as the Noether procedure, the Higgs mechanism, and the interactions involving light neutrinos. This is followed by extending the Standard Model by considering only one generation of light and heavy neutrinos and introducing the Type I Seesaw Model. The section concludes with a generalization up to three generations, involving the diagonalization of the mass matrix, and presenting the full Lagrangian density and Feynman rules of the HNL.

The second major section explores the phenomenological aspects of heavy neutrinos within the context of the FCC-ee collider. It includes an overview of the FCC-ee framework and examines both indirect and direct production mechanisms of heavy neutrinos. Detailed analyses cover decay width calculations, chirality and helicity properties, and limits on heavy neutrino masses. The section also investigates the flight distance of heavy neutrinos at FCC-ee.

The third section focuses on the detection and analysis of heavy neutrino signatures within the CLD detector. It outlines the production of Monte-Carlo samples, describes the CLD detector setup and simulation processes, and details the methods for reconstructing particle tracks. Additionally, this section identifies signal and background sources and evaluates the detector's sensitivity to various signatures of long-lived heavy neutrinos.

2 Building the theoretical model of heavy neutrinos

This section provides readers with a detailed summary of the theoretical framework underpinning these analyses. It includes a brief explanation of HNLs within the context of the phenomenological Type-I Seesaw model, which leads to both HNLs. You can find more details here [1, 2, 3, 4]

2.1 Reminder of the electroweak Standard Model

The Standard Model of particle physics is based on several fundamental principles:

- the space-time symmetry: the restricted Lorentz group and the time-space translation.
- the gauge symmetry: $SU(3)_C \times SU(2)_L \times U(1)_Y$ (C for colour, L for left-handed chirality and Y for weak hypercharge) before spontaneous symmetry breaking.
- the conditions of renormalizability: the Lagrangian density contains only operators with dimension 4 or less.

It is important to remind that there are also accidental symmetries such as the conservation of the global leptonic number L .

2.1.1 The Noether procedure

In our context, the QCD will not be taken into account, so the gauge symmetry will be $SU(2)_L \times U(1)_Y$. To simplify the description, we will consider only leptons and only one generation of leptons. With this assumptions, we have two leptons : an electron e a neutrino ν and the anti-particles associated.

For fermions, it is possible to define two chirality operators:

$$P_R = P_+ = \frac{1}{2}(1 + \gamma^5) \quad \text{and} \quad P_L = P_- = \frac{1}{2}(1 - \gamma^5)$$

The electron is the sum of the two possible chiralities :

$$e = P_L e + P_R e = e_L + e_R \quad \text{and} \quad \bar{e} = e^\dagger \gamma^0 = \bar{e} P_R + \bar{e} P_L = \bar{e}_R + \bar{e}_L$$

The neutrino is considered massless and the Goldhaber experiment [5] showed that there is only left-handed helicity neutrinos, so $\nu = \nu_L$ and $\bar{\nu} = \bar{\nu}_R$. We gather left-handed chiralities particles into doublets and right-handed chiralities into singlets.

The Lagrangian density corresponding to free massless electron and neutrino can be expressed as:

$$\mathcal{L}_{fermion} = \bar{L} i \gamma^\mu \partial_\mu L + \bar{e}_R i \gamma^\mu \partial_\mu e_R \quad \text{by writing} \quad L = \begin{pmatrix} \nu_L \\ e_L \end{pmatrix} \quad \text{and} \quad \bar{L} = (\bar{\nu}_L \quad \bar{e}_L)$$

The Noether procedure consists in making the theory invariant to a local $SU(2)_L \times U(1)_Y$ symmetry. To this goal, we need to replace the traditional derivative operator ∂_μ by a covariant derivative

$$D_\mu = \partial_\mu - ig' Y B_\mu - ig_W T_i W_i^\mu$$

where g' and g_W are respectively the gauge coupling of the $U(1)_Y$ group and $SU(2)_L$ group. Y and T_i are the generators of the $U(1)_Y$ group and $SU(2)_L$ group. Four gauge vector bosons, B_μ and W_i^μ , have been introduced and we need to add kinetic terms for them :

$$\mathcal{L}_{boson} = -\frac{1}{4} B_{\mu\nu} B^{\mu\nu} - \frac{1}{4} W_i^{\mu\nu} W_{\mu\nu}^i$$

The problem is that the gauge symmetry avoids us from adding a mass term for fermions. This mass term can be written by introducing the Higgs mechanism.

2.1.2 The Higgs mechanism and particle masses

The Higgs mechanism allows us to break the gauge symmetry $SU(2)_L \times U(1)_Y$ to the group $U(1)_{EM}$ which has the elementary charge e as gauge coupling. It requires the addition to the Lagrangian density of the following term:

$$\mathcal{L}_{Higgs} = (D_\mu \Phi)(D^\mu \Phi^\dagger) - V(\Phi) \quad \text{with} \quad V(\Phi) = \mu^2 \Phi^\dagger \Phi + \lambda^4 (\Phi^\dagger \Phi)^2$$

The parameters μ is a complex parameter such as $\mu^2 < 0$ and λ is a positive real. Φ is a complex scalar field doublet defined by: $\Phi = \begin{pmatrix} \Phi^+ \\ \Phi^0 \end{pmatrix}$ Now, we spontaneously break the gauge symmetry by choosing a particular case of Φ :

$$\Phi = \frac{1}{\sqrt{2}} \begin{pmatrix} 0 \\ v + h(x) \end{pmatrix}$$

where v is the vev (vaccum expectation value) and $h(x)$ is a scalar real field called the Higgs boson. The mass of the gauge bosons can be obtained by expanding the term $(D_\mu \Phi)(D^\mu \Phi^\dagger)$. For adding a mass to the electron, we implementing the Yukawa interaction term:

$$\mathcal{L}_{Yukawa} = -\frac{y_e}{\sqrt{2}} \bar{e}_R (\Phi^\dagger L_e) + h.c$$

The parameter y_e is the Yukawa parameter for the electron. By developping this term, we obtain a mass term for the electron: $m_e = \frac{y_e}{\sqrt{2}} v$. It is important to notice that there is no possibility to write a Yukawa term for the neutrino, that's why it is massless in the Standard Model.

2.1.3 Interactions involving the neutrino

The neutrino are involved in interactions through a Z^0 or a W^\pm boson. We remind that these bosons (interaction bosons) are linked to the gauge bosons by the Weinberg angle noted θ_W :

$$\begin{cases} A_\mu &= \cos \theta_W B_\mu + \sin \theta_W W_\mu^3 \\ Z_\mu &= -\sin \theta_W B_\mu + \cos \theta_W W_\mu^3 \end{cases} \quad \text{and} \quad W_\mu^\pm = \frac{1}{\sqrt{2}} (W_\mu^1 \mp i W_\mu^2)$$

By expanding the covariant derivative D_μ in the Lagrangian density piece $\mathcal{L}_{fermion}$, we obtain:

- the charged current with a trilinear interaction between a W^\pm boson, an electron and neutrino:

$$\mathcal{L}_{W e \nu} = -\frac{e}{\sqrt{2} \sin \theta_W} W_\mu^- \bar{\nu} \gamma^\mu P_L e^-$$

- the neutral current with a trilinear interaction between a Z^0 boson, a neutrino and an anti-neutrino:

$$\mathcal{L}_{Z \nu \nu} = -\frac{g_W}{\cos \theta_W} Z_\mu \bar{\nu} \gamma^\mu (c_L P_L + c_R P_R) \nu \quad \text{with} \quad c_L = +1/2 \quad \text{and} \quad c_R = 0$$

2.2 Extending the Standard Model with one generation of light and heavy neutrinos

The neutrinos oscillation observation [6] [7] can be only explained if the neutrinos are massive. We will study the different possible mass terms for a neutrino and propose a consistent theory.

2.2.1 Dirac and Majorana mass terms

In the Standard Model, Lorentz invariance, gauge invariance and renormability must be respected. For a fermion with zero charge, there are two Lorentz invariant possibilities :

- 1) **Dirac term:**

$$\mathcal{L}_{Yukawa} = -\frac{y_\nu}{\sqrt{2}} \bar{\nu}_R (\tilde{\Phi}^\dagger L) + h.c \implies -m_\nu \bar{\nu} \nu - \frac{y_\nu}{\sqrt{2}} h(x) \bar{\nu} \nu$$

This term is gauge invariant and renormalisable. But the problem is that ν_R does not exist. If we add it, there would be an interaction between W and ν_R , and the Goldhaber experiment should have given half right-handed, half left-handed neutrinos. Furthermore, there is no explanation for Yukawa's small term compared to other particles.

2) Majorana term:

$$\mathcal{L}_{Majorana} = -m\bar{\nu}_L(\nu_L^c) + h.c \implies -m_\nu\bar{\nu}\nu$$

In this case, $\nu = \nu_L + \nu_L^c$; ν_L^c the charge conjugate of ν_L (neutrinos do not have charge but it inverses also the leptonic number). But there are some problems with this term. First, it works only if $\nu_L^c = \nu_L$, it means Majorana spinor and there is no experimental proof of that. Second, there is a total leptonic number violation ($\Delta L = 2$). And third, this term is not gauge invariant (like the Dirac mass) and we need to find a gauge invariant expression which generates it after the spontaneous breaking symmetry. This term exists and it is called the Weinberg operator [8] but it has dimension equal to 5. So the term is not renormalizable.

2.2.2 Masses in in the framework of type-I Seesaw Model

The Seesaw model combines the two possible mass terms for a electrically-neutral fermions. As discussed before, it violates the total leptonic number and it is not renormalizable. This model introduces a new neutrino noted N_R which has a right chirality. Besides, this neutrino is singlet under the SM gauge symmetry (no color, weak isospin, or weak hypercharge charges). Thus the most general mass term can be expressed as:

$$\begin{aligned} -\mathcal{L}_{\nu \text{ mass}} = & -m_D(\bar{N}_R\nu_L + \bar{\nu}_L N_R) && \text{Dirac} \\ & -\frac{m_L}{2}(\bar{\nu}_L^c\nu_L + \bar{\nu}_L\nu_L^c) && \text{Majorana for } \nu_L \\ & -\frac{m_R}{2}(\bar{N}_R^c N_R + \bar{N}_R N_R^c) && \text{Majorana for } N_R \end{aligned}$$

m_D is the Dirac mass whereas m_L and m_R are respectively the Majorana mass for the light and the heavy neutrinos. These masses can be combined into a neutrino mass matrix as:

$$-\mathcal{L}_{\nu \text{ mass}} = \frac{1}{2} \begin{pmatrix} \bar{\nu}_L^c & \bar{N}_R \end{pmatrix} \mathcal{M}_\nu \begin{pmatrix} \nu_L \\ N_R^c \end{pmatrix} + h.c \quad \text{with} \quad \mathcal{M}_\nu = \begin{pmatrix} m_L & m_D \\ m_D & M_R \end{pmatrix}$$

As discussed before, m_L is taken to zero. We obtain the final mass term by diagonalizing \mathcal{M}_ν (possible because real symmetric): $\mathcal{M}_\nu = V\mathcal{D}_\nu V^T$ with V a real direct (determinant equal to +1) orthogonal matrix which can be interpreted as a planar rotation of angle θ . After diagonalizing:

$$\mathcal{D}_\nu = \begin{pmatrix} m & 0 \\ 0 & M \end{pmatrix} \quad \text{and} \quad V = \begin{pmatrix} \cos\theta_N & \sin\theta_N \\ -\sin\theta_N & \cos\theta_N \end{pmatrix}$$

$$\text{with } m, M = \frac{1}{2} \left((m_L + m_R) \mp \sqrt{(m_L - m_R)^2 + 4m_D^2} \right) \quad \text{and} \quad \tan(2\theta_N) = \frac{2m_D}{m_R - m_L}$$

The Lagrangian density for the neutrinos can be written after diagonalization as:

$$-\mathcal{L}_{\nu \text{ mass}} = m\bar{\nu}\nu + M\bar{N}^c N \quad \text{with} \quad \begin{pmatrix} \nu_L \\ N_R^c \end{pmatrix} = V \begin{pmatrix} \nu \\ N^c \end{pmatrix}$$

For the situation $m_L = 0$ (Dirac standard neutrino) and $m_R \gg m_D$, the neutrino masses are :

$$m \approx \frac{m_D^2}{m_R} \quad \text{and} \quad M \approx m_R \left(1 - \frac{m_D^2}{m_R^2}\right) \approx m_R$$

Thus the Seesaw mechanism provides a neutrino with a low mass (the one that we observe) and a neutrino with a high mass (not observed yet). By introducing a right-handed chirality neutrino with a large Majorana mass m_R , it explains why the mass of the light neutrino is so small.

2.2.3 Interactions in in the framework of type-I Seesaw Model

First, adding a heavy neutrino N_R in the theory implies that a corresponding kinematic term $\bar{N}_R i\gamma^\mu D_\mu N_R$ must be added to $\mathcal{L}'_{fermion}$. As the right-handed neutrino has no charge at all, the covariant derivative D_μ is equal to the traditional ∂_μ . Therefore, no interaction between the gauge bosons and the right-handed neutrino can be generated by Lagrangian term, contrary to the light neutrinos. This statement motivates the name of *sterile neutrino*.

Second, the Standard Model described in section 2.1.3 was written in terms of interaction states. They must be rewritten in term of mass states by using the matrix of passage V : $\nu_L = \cos \theta_N \nu + \sin \theta_N N^c$

- the charged current with a trilinear interaction between a W^\pm boson, an electron and heavy neutrino:

$$\mathcal{L}'_{We\nu} = -\frac{e \sin \theta_N}{\sqrt{2} \sin \theta_W} W_\mu^- \bar{N}^c \gamma^\mu P_L e^-$$

- the neutral current with a trilinear interaction between a Z^0 boson, a light neutrino and a heavy anti-neutrino:

$$\mathcal{L}'_{ZN\nu} = -\frac{g_W \sin \theta_N}{2 \cos \theta_W} Z_\mu \bar{N}^c \gamma^\mu P_L \nu$$

- the neutral current with a trilinear interaction between a Z^0 boson, a heavy neutrino and a heavy anti-neutrino can be neglected because the term is proportional to $\sin^2 \theta_N$.

Finally, we remind that the Dirac mass term can be derived from the Weinberg operator after the spontaneous symmetry breaking. To the addition of the mass term, the Weinberg operator generates an interaction term between the Higgs and the neutrinos:

$$\mathcal{L}'_{hN\nu} = -\frac{g_W m_N \sin \theta_N}{2M_W} h \bar{N}^c P_L \nu$$

2.3 Generalization to three generations of leptons

The complete model extends the Standard Model (with three generation of leptons) field content by introducing three right-handed chirality neutrinos noted N_{H_1} , N_{H_2} and N_{H_3} . The most general mass term can be expressed by a 6×6 mass matrix \mathcal{M}_ν . As this matrix is symmetric, it can be diagonalized. The interaction states and mass states are linked by the matrix of passage:

$$\begin{pmatrix} \nu_{L_i} \\ N_{R_i}^c \end{pmatrix} = \begin{pmatrix} U_{3 \times 3} & V_{3 \times 3} \\ X_{3 \times 3} & Y_{3 \times 3} \end{pmatrix} \begin{pmatrix} \nu_i \\ N_i^c \end{pmatrix}$$

The U matrix describes the mixing between the light neutrinos and it is called the PMNS matrix (Pontecorvo-Maki-Nakagawa-Sakata). We consider that U is the identity for simplicity in the following. The V matrix described the mixing between active and sterile neutrinos.

Concerning the interaction, the Lagrangian density terms have been gathered in the following formula [9, 10]:

$$\begin{aligned} \mathcal{L}_{Int} = & -\frac{g_W}{\sqrt{2}} W_\mu^- \sum_{k=1}^3 \sum_{\ell=e}^{\tau} \bar{N}_k^c V_{\ell k}^* \gamma^\mu P_L \ell - \frac{g_W}{\sqrt{2}} W_\mu^+ \sum_{k=1}^3 \sum_{\ell=e}^{\tau} \bar{\ell} V_{\ell k} \gamma^\mu P_L N_k^c \\ & - \frac{g_W}{2 \cos \theta_W} Z_\mu \sum_{k=1}^3 \sum_{\ell=e}^{\tau} \bar{N}_k^c V_{\ell k}^* \gamma^\mu P_L \nu_\ell - \frac{g_W}{2 \cos \theta_W} Z_\mu \sum_{k=1}^3 \sum_{\ell=e}^{\tau} \bar{\nu}_\ell V_{\ell k} \gamma^\mu P_L N_k^c \\ & - \frac{g_W m_N}{2 M_W} h \sum_{k=1}^3 \sum_{\ell=e}^{\tau} \bar{N}_k^c V_{\ell k}^* P_L \nu_\ell - \frac{g_W m_N}{2 M_W} h \sum_{k=1}^3 \sum_{\ell=e}^{\tau} \bar{\nu}_\ell V_{\ell k} P_R N_k^c \end{aligned}$$

From this interaction Lagrangian density, we deduce the Feynman rules that will be useful for the computations. All the Feynman rules can be found in Appendix A.

2.4 Experimental constraints

Determining the experimental constraints on the model parameters requires a deep review of all experimental measures and requires to take some precaution on the theoretical assumption taken. This complex study has not been done during this internship. But we would like to highlight some important results. Considering only one generation of heavy neutrino, the model parameters are $\sin \theta_N$ and m_N .

First the model parameters must be consistent with the Seesaw mechanism *i.e* they should give small masses to light neutrinos. Considering an order of magnitude of 10^{-1} eV for the light neutrino masses, we derive a first constraint: $m_N \sin^2 \theta_N > 10^{-1}$ eV in order to avoid from too small mass for neutrinos. This is the so-called *SeeSaw bottomline*. Besides, the neutrino masses can not be too large (in particular the Dirac mass m_D) that's why we expect that the Yukawa coupling must be smaller than 1. So we derive a second constraint: $v \sin^2 \theta_N / m_N < 1$. Thus, the allowed region of parameter-space is given by Figure 1.

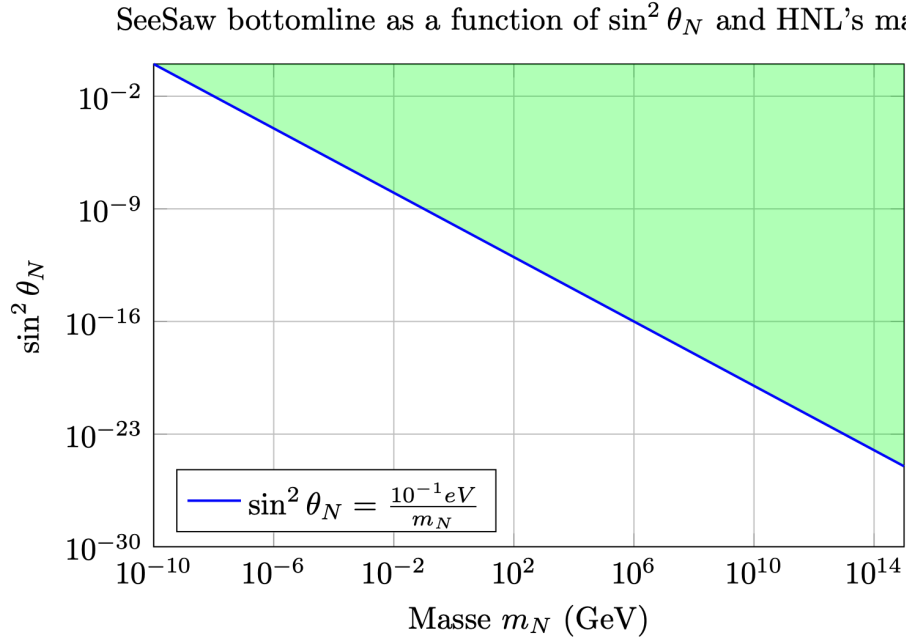


Figure 1: SeeSaw bottomline

The experiences which can constrain the model parameters by their measures can be classified according to the value of the m_R mass. Fixed target experiments are sensible to m_R values less than 1 GeV. Electron-Positron colliders can probe the range of mass up to the electroweak boson masses. The best limits excludes the region up to $\sin^2 \theta_N \approx 10^{-5}$. Below the Z mass, the hadronic colliders are fiercely more sensible. For instance, the CMS experience has managed to exclude from $m_N = 100$ GeV up to $\sin^2 \theta_N \approx 10^{-2}$ to $m_N = 1$ TeV up to $\sin^2 \theta_N \approx 1$ [11]. These experimental constrains should be relaxed if we consider several generation of heavy neutrinos.

3 Study of the heavy-neutrinos phenomenology at FCC-ee

As the model has been built and the Feynman rules for the interaction vertices have been derived, we would like to study how the heavy neutrino can be produced at the FCC-ee collider and what are the possible decay channels. We will focus on the region of parameter space for which the heavy neutrino is long-lived.

3.1 Framework of the study

3.1.1 The FCC-ee

The FCC-ee is part of a larger Future Circular Collider initiative, which includes plans for various collider types to be built within a 100 km circular tunnel in the Geneva region

as show Figure 2. This ambitious project seeks to build upon the successes of the Large Hadron Collider (LHC) by creating a next-generation electron-positron collider.

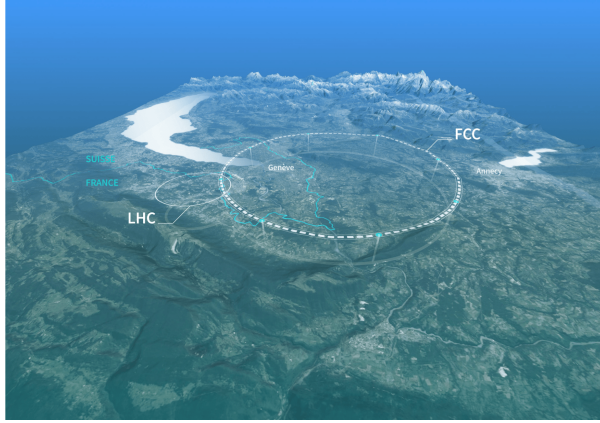


Figure 2: Artist's view of the future FCC

This initial phase, referred to as the FCCee-Z, is designed to operate at an energy level of 91 GeV, which is the precise mass of the Z boson. Scrutinizing around the Z pole allows scientists to produce vast quantities of Z bosons, facilitating detailed studies of their properties with unprecedented precision. The FCCee-Z will serve as a high-luminosity machine, generating a large number of Z bosons. This abundance of data is expected to provide new insights into electroweak interactions, rare decay processes, and possible signs of new physics beyond the Standard Model.

3.1.2 Simplified assumptions on the model

In order to simplify the model, we consider a diagonal matrix for the mixing matrix V : $V = \text{diag}(V_1, V_2, V_3)$ with $|V_1|^2 + |V_2|^2 + |V_3|^2 = 1$ due to the unitary condition. Therefore no violation of partial leptonic number is allowed. We focus only the first generation of neutrinos, so the coupling involved in the following will be V_1 that we noted V for simplicity. Thus the model depends only on two parameters: the coupling V and the mass of the heavy neutrino m_N . Finally, the calculation of cross-sections and decay widths will be performed in the ultra-relativistic conditions *i.e* the mass of the electron and light neutrinos are negligible compared to the momentum values.

3.1.3 Techniques of calculation

The expression of the different cross-section and decay widths have been derived by hand. We remind here the different steps:

- We derive the matrix element $i\mathcal{M}$ associated with the Feynman diagram of the process by using the Feynman rules of the model.
- We calculate the square modulus $|\mathcal{M}|^2$ of the element of matrix.
- The final states have a polarization and we sum on all the polarization states in order to include all the possibilities. Concerning the polarization of the initial particle (except for the Higgs boson which is scalar), we do not favour a particular state by calculating the average on the polarization states. averaged, so this has to be taken into account. The obtained square modulus is noted $|\overline{\mathcal{M}}|^2$.

- This term can be expressed in terms of traces of Dirac matrices by using the Casimir's trick. All the trace identities used can be found in Appendix C.
- Then we can apply the cross section formula or the decay width formula available in the center-of-mass frame. For example, the decay width expression adapted for 1×2 processes in center-of-mass frame:

$$\frac{d\Gamma^*}{d\Omega^*} = \frac{1}{64\pi^2 M^3} \sqrt{\lambda(M^2, m_1^2, m_2^2)} |\overline{\mathcal{M}}|^2$$

where M is the mass of the incoming particle, m_1 and m_2 the masses of the two created particles and λ the Källén function.

- The full cross-section or decay width is obtained by integrating over the solid angle.

The chirality analysis has been performed by tuning the calculation technique. Indeed, we separate a Dirac spinor Ψ into a left-handed chirality Ψ_L and a right-handed chirality fermions Ψ_R by using the chirality projectors:

$$P_R = \frac{1}{2}(1 + \gamma^5) \quad \text{and} \quad P_L = \frac{1}{2}(1 - \gamma^5)$$

The helicity analysis has been performed in the same way than the chirality analysis. The difference is coming from the definition of the projectors defined below. We remind that the helicity is not a Lorentz invariant because the boosts do not generally preserve helicity. The study is therefore dependent of the frame and we choose the center-of-mass frame for the study.

$$H_R(s) = \frac{1}{2}(1 + \gamma^5 \not{s}) \quad \text{and} \quad H_L(s) = \frac{1}{2}(1 - \gamma^5 \not{s}) \quad \text{with} \quad \not{s} = s_\mu \gamma^\mu \quad \text{and} \quad s = \left(\beta\gamma, \gamma \frac{\vec{\beta}}{\beta} \right)$$

3.1.4 Validation of the results

All the cross-sections and the decay widths have been calculated by hand. The numerical values have been cross-checked with the Monte-Carlo MADGRAPH_AMC@NLO [12] using the FEYNRULES model available here [9].

3.2 Indirect production of the heavy neutrinos

First, we will look at the case of indirect production of heavy neutrinos *i.e* the production in the decay of the known elementary bosons (the Z^0 , the W^\pm and the Higgs boson). This mode of production is allowed if the mass of the heavy neutrino is smaller than the mass of the decaying boson.

3.2.1 Decay width calculation

We consider the three processes illustrating by Figure 3. By calculation, we derive the analytical formulae of the partial decay widths given below.

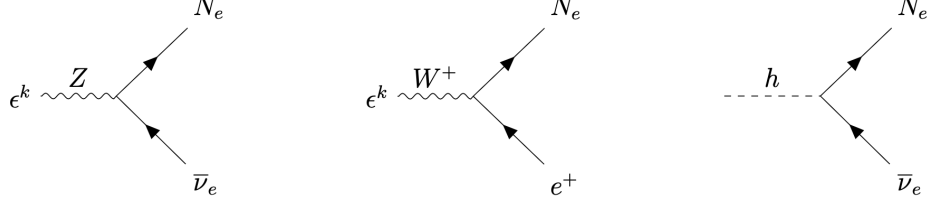


Figure 3: Feynman diagrams describing the decay of standard bosons with a heavy neutrino in the final states

$$\begin{aligned}\Gamma(Z \rightarrow N_e \bar{\nu}_e) &= \frac{g_Z^2 |V|^2 m_Z}{192 \pi} \left(\left(1 - \frac{m_N^2}{m_Z^2}\right)^2 + \left(1 - \frac{m_N^2}{m_Z^2}\right) \left(1 - \frac{m_N^4}{m_Z^4}\right) \right) \\ \Gamma(W^+ \rightarrow N_e e^+) &= \frac{g_W^2 |V|^2 m_W}{92 \pi} \left(\left(1 - \frac{m_N^2}{m_W^2}\right)^2 + \left(1 - \frac{m_N^2}{m_W^2}\right) \left(1 - \frac{m_N^4}{m_W^4}\right) \right) \\ \Gamma(h \rightarrow N_e \bar{\nu}_e) &= \frac{g_W^2 |V|^2}{64 \pi m_W^2} m_N^2 m_h \left(1 - \frac{m_N^2}{m_h^2}\right)^2\end{aligned}$$

The decay width for the channel $W^+ \rightarrow N_e e^+$ is very similar to the traditional channel $W^+ \rightarrow \nu_e e^+$. If we take $|V|^2=1$ and a massless N_e , the values of the decay widths are exactly equal. The expression of the decay width for the channel $Z \rightarrow N_e \bar{\nu}_e$ is equivalent to the $W^+ \rightarrow N_e e^+$ up to a factor and the mass replacement. This result differs from the Standard model in which the Z boson decays always in two fermions of same masses. We can notice that taking $|V|^2 = 1$ and a massless N_e gives the standard value of the decay width corresponding to the channel $Z \rightarrow \bar{\nu}_e \nu_e$. For the Higgs boson decay, the masses of the final are different and the decay width is not proportional to the mass of a particle.

Figure 4 shows the evolution of the decay width as a function of the heavy neutrino mass. For the W and the Z bosons, the decay width value decreases with the heavy neutrino mass. Larger the neutrino mass is, smaller the probability to produce a heavy neutrino is. For the Higgs boson, the decay width is null for a massless heavy neutrino. It increases with the mass up to reach a maximum obtained at a mass equal to $m_H/\sqrt{3}$ and then decreases.

3.2.2 Chirality and helicity analysis

In order to get a better understanding of the decay width expression, we proceed to a chirality analysis and a helicity analysis. Tables 1 and 2 provide the calculated fraction of each chirality/helicity combination. All the contribution of these combinations have calculated by hand.

For the chirality analysis, only one combination is allowed for each decay process. We have a vector-axial coupling for the Z and the W decay. This structure authorized only a right-handed chiral $\bar{\nu}_e$ and a left-handed chiral N_e^c (we remind that N_e is right-handed chiral whereas N_e^c is left-handed chiral). The coupling to the Higgs is pseudoscalar and can only link a right-handed chiral $\bar{\nu}_e$ and a right-handed handed chiral N_e .

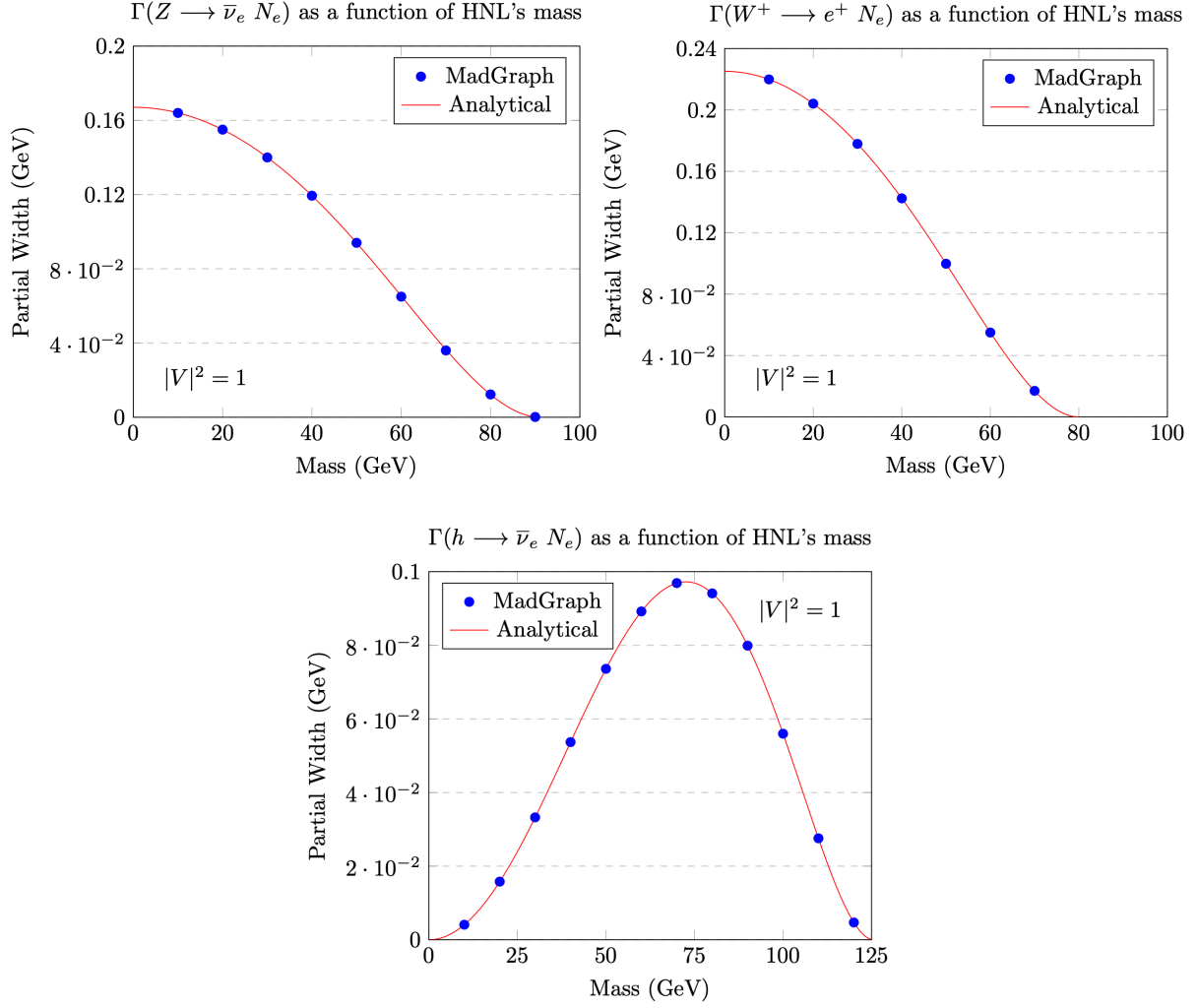


Figure 4: Plot of analytical formulas for decay widths and numerical values obtained with MADGRAPH_AMC@NLO

The helicity analysis is quite similar to the chirality analysis. The results are exactly the same if the final states are massless (chirality states are exactly equal to helicity states). For the Z and W decays, the proportion of both right-handed helicity $\bar{\nu}_e$ and N_e is non null for a massive N_e . As illustrates Figure 5, in the center-of-mass frame, the proportion increases with the mass and the maximum ($1/3 \approx 33\%$) is reached when the mass is equal to the decaying boson mass. For the Higgs decay, there is no contribution with left-handed helicity N_e because the Higgs boson has a null spin.

3.2.3 Limit on the heavy neutrino mass and mixing term

The fact that the studied decays have never been observed suggests that these partial decay widths are smaller than the experimental uncertainty on the estimation of the total decay widths of these bosons. We remind the updated values of total decay widths estimated by the Particle Data Group collaboration [13]:

	N_e	$\bar{\nu}_e$	%		N_e	$\bar{\nu}_e$	%
For Helicity:	R	R	100	For Chirality:	R	R	100
	R	L	0		R	L	0
	L	R	0		L	R	0
	L	L	0		L	L	0

Table 1: Contribution in % to the partial decay width of the Higgs boson of the fermion helicity combinations (left) and of the fermion chirality combinations (right)

	N_e	$\bar{\nu}_e$	%		N_e	$\bar{\nu}_e$	%
For Helicity:	R	R	$\frac{x^2}{2+x^2}$	For Chirality:	R	R	0
	R	L	0		R	L	0
	L	R	$\frac{2}{2+x^2}$		L	R	100
	L	L	0		L	L	0

Table 2: Contribution in % to the partial decay width of the Z boson of the fermion helicity combinations (left) and of the fermion chirality combinations (right). In the equation x corresponds with the ratio m_N/m_Z .

Contribution to $\Gamma(Z \rightarrow N_e \bar{\nu}_e)$ of $N_e \bar{\nu}_e$ helicity combination

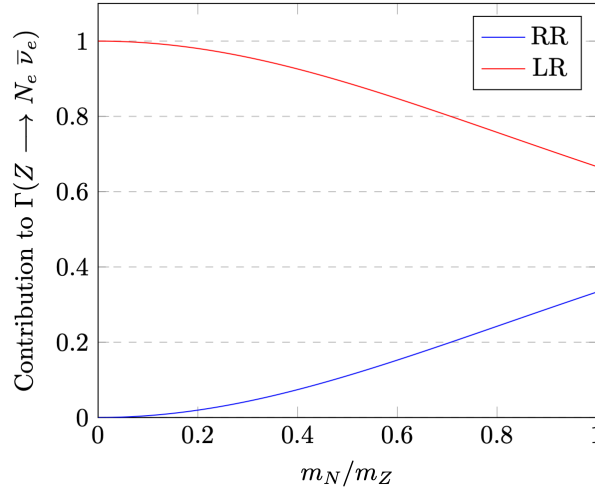


Figure 5: Contribution to $\Gamma(Z \rightarrow N_e \bar{\nu}_e)$ of $N_e \bar{\nu}_e$ helicity combination

- $\Gamma_Z = (2.4955 \pm 0.0023) \text{ GeV}$
- $\Gamma_W = (2.085 \pm 0.042) \text{ GeV}$
- $\Gamma_H = 3.7_{-1.4}^{+1.9} \text{ MeV}$

Since the two unknown parameters for the HNL model are the mixing term $|V|^2$ and the mass m_N , we can extract the value range of these two parameters consistent with the uncertainty on the total decay widths. Figure 6 shows by a curve the required conditions in order to have a partial decay width equal to the uncertainty on the total decay width.

The allowed region of parameter spaces is the region under the curves. We conclude that the Z total decay width is the most constraining due to the accuracy of experimental uncertainty. For small HNL masses, the mixing parameter $|V|^2$ must be smaller than 10^{-2} . It is less constrained at high mass values. For a HNL mass of 75 GeV, it should be smaller than 10^{-1} .

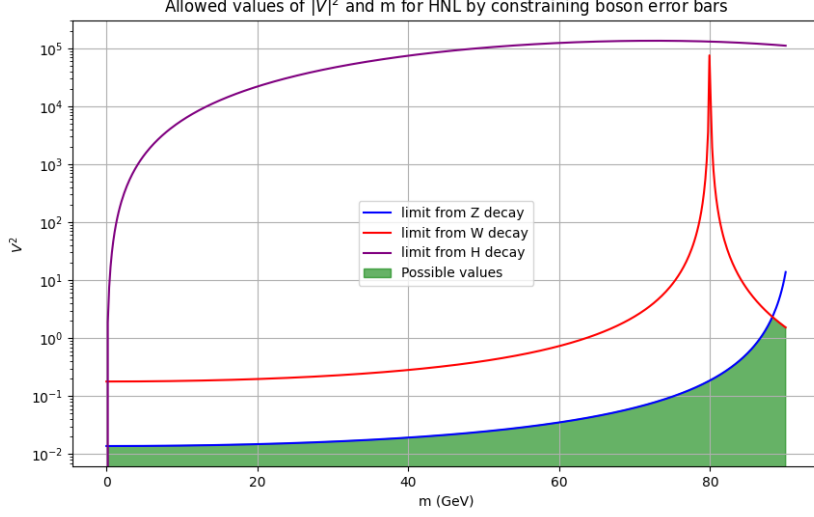


Figure 6: Region of the model parameter space not constrained by the measure of the total decay width of the Z , W and Higgs bosons.

3.3 Direct production of the heavy neutrinos

In this section, we are interested in the direct production of the heavy neutrinos *i.e.* coming from the e^+e^- collision at the FCCee. We focus on the final states N_e and ν_e . This process can be carried out at the Leading order of the electroweak theory in three ways, as shown in the Feynman diagrams of Figure 7: via a Z or an h in the s -channel, and via a W in the t -channel.

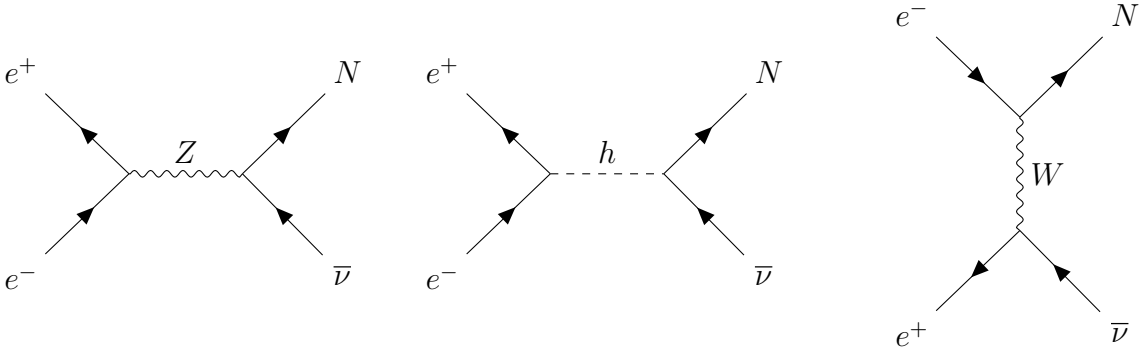


Figure 7: The Feynman diagrams describing the production process at the Leading-Order of the theory

The total element of matrix $i\mathcal{M}$ is the sum of the individual elements corresponding

to each diagram and by taking into account a possible relative sign between the diagrams:

$$i\mathcal{M}_{tot} = i\mathcal{M}_Z + i\mathcal{M}_h - i\mathcal{M}_W$$

This expression lead to a total cross section which can be split into several pieces:

$$\sigma_{tot} = \sigma_Z + \sigma_W + \sigma_h - \sigma_{W/Z} - \sigma_{W/h} + \sigma_{Z/h}$$

The three first cross-sections are related to the amplitude of an individual diagram ; the three last one are related to the interferences term. By calculation we derive the expression of the different cross-section pieces depending on the parameters of the model but also the :

- $\sigma_Z = \frac{e^4 |V|^2 ((c_L^e)^2 + (c_R^e)^2) s}{1536 \pi \cos^4 \theta_W \sin^4 \theta_W \left((s - m_Z^2)^2 + (m_Z \Gamma_Z)^2 \right)} (r^2 + 2) (1 - r^2)^2$
- $\sigma_h = \frac{g_W^4 |V|^2 m_e^2 s^2}{512 \pi m_W^4 \left((s - m_h^2)^2 + (m_h \Gamma_h)^2 \right)} r^2 (1 - r^2)^2$
- $\sigma_W = \frac{g_W^4 |V|^2}{128 \pi s} \left[2(1 - r^2) + (2 - r^2 + 2r_W^2) \ln \left(\frac{r_W^2 (r_W^2 + \gamma_W^2)}{((1 - r^2) + r_W^2)^2 + r_W^2 \gamma_W^2} \right) \right. \\ \left. + 2 \frac{-r^2(1 + r_W^2) + (1 + 2r_W^2) + r_W^2 (r_W^2 - \gamma_W^2)}{r_W \gamma_W} \cdot \left(\arctan \left(\frac{(1 - r^2) + r_W^2}{r_W \gamma_W} \right) - \arctan \left(\frac{r_W}{\gamma_W} \right) \right) \right]$
- $\sigma_{W/h} = \sigma_{Z/h} = 0$
- $\sigma_{WZ} = \frac{e^2 |V|^2 c_L^e g_W^2}{128 \pi \cos^2 \theta \sin^2 \theta} \cdot \frac{1}{s} \cdot \frac{\left(1 - \frac{m^2}{s}\right) (m^2 - s)}{(s - m_Z^2)^2 + m_Z^2 \Gamma_Z^2} \\ \cdot \int_{-2}^0 dx \frac{\left(s - \frac{1}{2}x(m^2 - s)\right) \left(\frac{1}{2}x + 1\right) \left(\frac{1}{2}x(m^2 - s)(m_Z^2 - s) - sm_W^2 + m_W m_Z \Gamma_W \Gamma_Z + m_W^2 m_Z^2\right)}{\left(m_W^2 + \frac{1}{2}x(m^2 - s)\right)^2 + m_W^2 \Gamma_W^2}$

with $r = \frac{m_N}{\sqrt{s}}$, $r_W = \frac{m_W}{\sqrt{s}}$ and $\gamma_W = \frac{\Gamma_W}{\sqrt{s}}$, $c_L^e = -\frac{1}{2} + \sin^2 \theta_W$ and $c_R^e = \sin^2 \theta_W$

Figure 8 shows the evolution of the components of the cross-sections as a function of the heavy neutrino mass at $\sqrt{s} = 91$ GeV. Figure 9 shows the total cross-section obtained by summing the different terms.

We notice first that the diagram with a Z mediation is the dominant with respect to the other. In fact, this result can be expected. The s-channel will inevitably be more influential, even if the \sqrt{s} is at Z-pole level (1st phase at FCCee) and the mass of the W should favour it. But the t-channel, because of its propagator, is greatly diminished. In addition, the interference term between the Z and the W has the same order of magnitude. In the case of the Higgs, it will be very negligible because the coupling to the electrons is very weak (small electron Yukawa coupling).

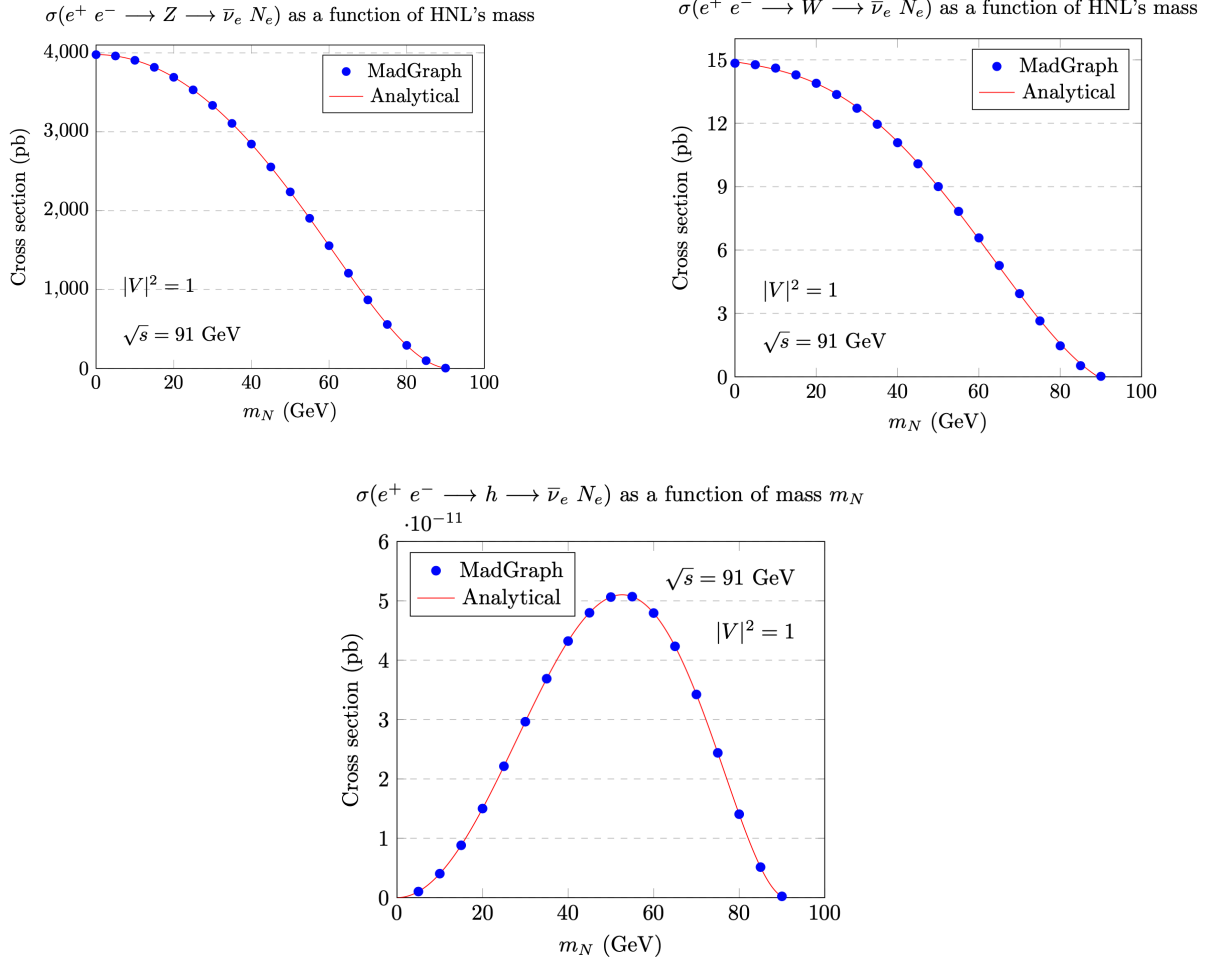


Figure 8: Plots of the different parts of the cross-sections (except for the interference terms): σ_h , σ_Z and σ_W .

3.4 Decay of the heavy neutrinos

In this section, we would like to study the decay of the heavy neutrino. As heavy neutrino with a mass less than 91 GeV can be produced at the FCCee, we must consider only the decay channels into fermions. Following the derived Feynman rules, this exotic particle can decay into fermions only by a Z , a W^\pm or h boson. If the heavy neutrino has a mass smaller than these bosons, the boson involved in the decay must be necessarily off-shell. In this case, the decay width is expected to be small and the particle could have a long-life time. The possible decay channels for the heavy neutrino are $\nu_e l^+ l^-$, $\nu_e q \bar{q}$, $e^- u \bar{d}$ and 3ν . As an example, the figure 10 show the different possible kinds of Feynman diagrams which can give the final state $\nu_e e^+ e^-$. The corresponding decay width has been calculated by hand (only for the Z mediation) and the result is given below.

$$\Gamma = \frac{g_Z^4 (V_{lk})^2 (C_L^2 + C_R^2)}{8 \cdot 32 M^3 \cdot (2\pi)^3} \int_{x=0}^{M^2} x (M^2 - x) \int_{y=0}^{M^2-x} \frac{1}{(y - m_Z^2)^2 + (m_Z \Gamma_Z)^2} dx dy$$

The total decay width has been calculated by MADGRAPH_AMC@NLO and the values are given in Figure 11 in the $|V|^2$ and m_R plane. As all the partial decay widths are proportional to $|V|^2$, the branching ratios are totally independent on $|V|^2$ and depends

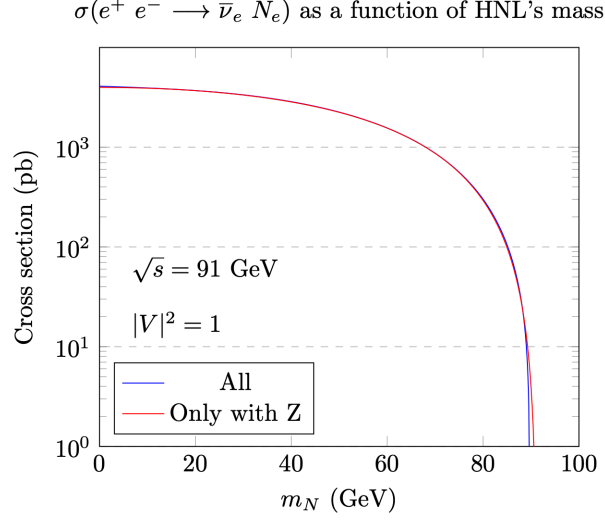


Figure 9: Cross section of the full process as function of the mass and comparison with the cross-section of Z-channel.

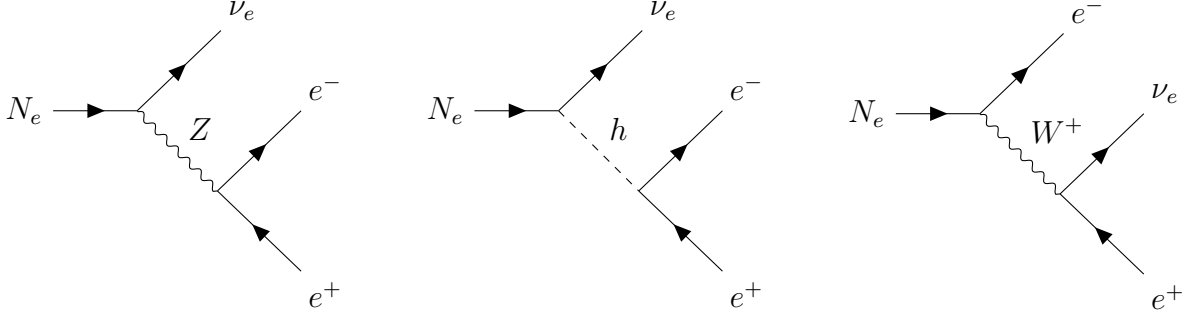


Figure 10: Feynman diagrams leading to the decay of the heavy neutrino to the final state $\nu_e e^+ e^-$

on m_R . Figure 11 show the branching ratio $\text{BR}(N_e \rightarrow e^+ e^- \nu_e)$ as a function of the mass m_N .

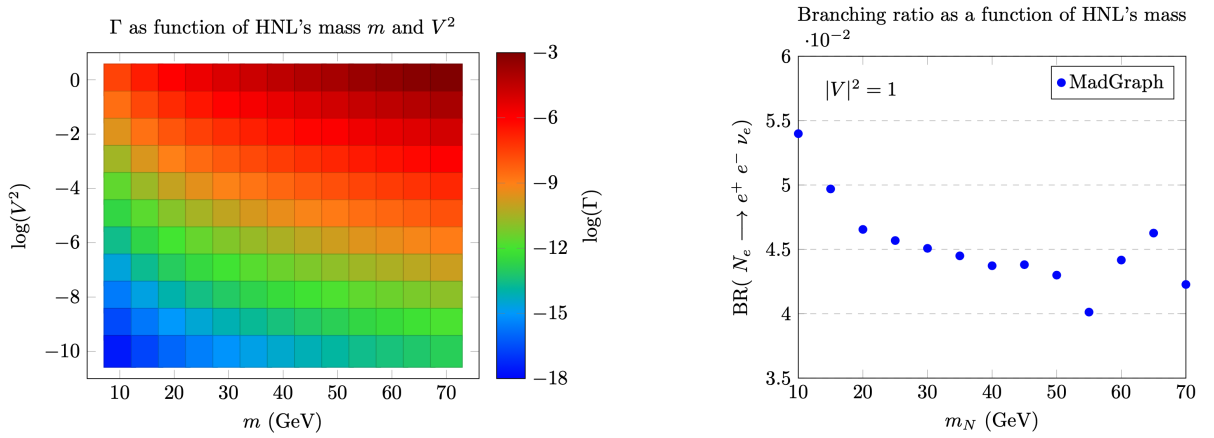


Figure 11: Full decay width of the heavy neutrino (left) and branching ratios of its decay channel (right)

3.5 Flight distance of the heavy neutrinos at FCC-ee

We are interested in the heavy neutrinos which are long-lived. We need to compute the lifetime and the mean flying distance of the particle. We remind the lifetime τ is linked to the total decay width Γ of the particle by the formula:

$$\tau = \frac{\hbar}{\Gamma}$$

The mean distance $\langle d \rangle$ traveled by the particle in the laboratory frame can be calculated by the formula:

$$\langle d \rangle = \beta\gamma c\tau$$

where $\beta = v/c$ and $\gamma = 1/\sqrt{1 - \beta^2}$ are the traditional relativistic parameters associated to the heavy neutrino. If we consider the scenario of direct production of the heavy neutrino, their product can be derived:

$$\beta\gamma = \frac{p_N}{m_N} = \frac{s - m_N^2}{2m_N\sqrt{s}}$$

The evolution of the relativistic factor $\beta\gamma$ is showed by the first plot of Figure 12. This factor is important at low mass. For instance, $\beta\gamma \approx 4$ for a mass of 10 GeV. For the range of mass [20 GeV ; 90 GeV], the average value of $\beta\gamma$ is around 1.0.

The final result is the second plot of Figure 12. It shows the average distance $\langle d \rangle$ traveled by the heavy neutrino in the plane $m_R - |V|^2$. We see a region where $\langle d \rangle$ is larger to 1 cm and can reach 1 m. FCCee is sensible to this range. It corresponds to the green zone on the figure.

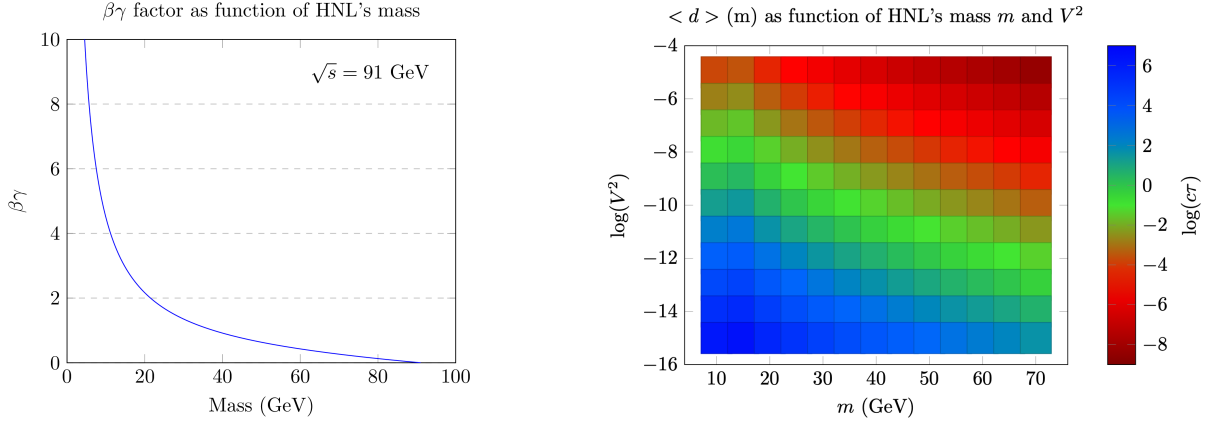


Figure 12: $\beta\gamma$ factor of the heavy neutrino in the direct production for $\sqrt{s} = 91$ GeV(left) ; Mean distance traveled by the heavy neutrino in the laboratory frame in meter (right)

4 Signature of a long-lived heavy neutrino in the CLD detector

4.1 Signal and background sources

During this internship, we choose as signal process the production at the FCC-ee of a HNL decaying into a pair of electrons and a light neutrino. Figure 13 shows the Feynman diagrams corresponding with the chosen signal. We define also several benchmark points. These points depend on the HLN mass: 10, 30 and 50 GeV. Instead of using the mixing parameter in the definition of the benchmark, we prefer working with the lifetime $c\tau$ (more exactly the flight distance in the proper frame of the HNL). The used values are: 1, 10 and 100 cm.

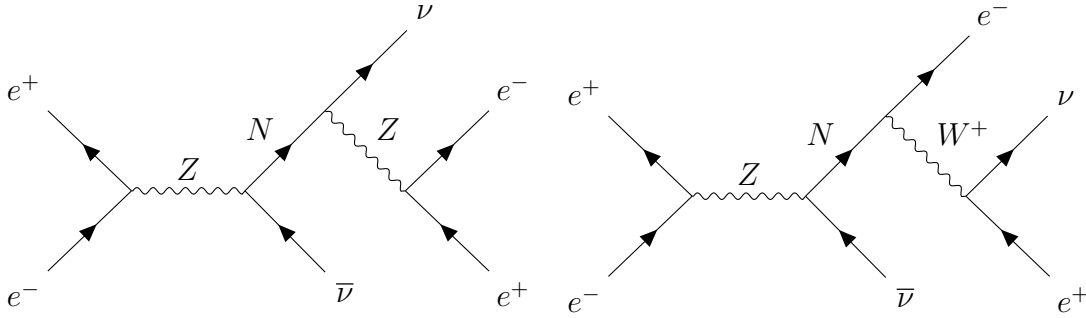


Figure 13: Feynman diagrams of HNL processes at electron-positrons collisions, with HNL production mediated with a Z boson, and HNL decays with a Z or W boson.

Several background sources can be enumerated. As an example, we can cite the production of a tau pair where the taus decay into an electron and neutrinos.

4.2 Production of Monte-Carlo samples

We produced a small sample of 200 events for each benchmark point. To this purpose, the MADGRAPH_AMC@NLO v3.5.3 [12] package was used for generating the hard process, combined to the model implementation SM_HEAVYN_CKM_ALLMASSES [9]. PYTHIA is used to simulate the final state radiation, the parton shower, the hadronization and the decay of unstable particles. Finally, the package DELPHES [14] is designed to simulate the response of the CLD detector.

4.3 The CLD detector and detector simulation

This detector [15] is derived from the most recent CLIC detector model, which features a silicon pixel vertex detector and a silicon tracker, followed by highly granular calorimeters (a silicon-tungsten ECAL and a scintillator-steel HCAL). A superconducting solenoid provides a strong magnetic field, and a steel yoke interleaved with resistive plate (RPC) muon chambers closes the field. Figure 14 shows an illustration of the detector.

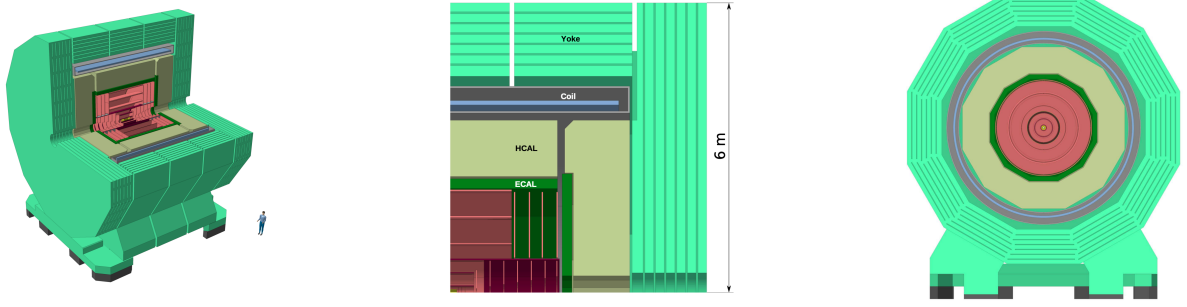


Figure 14: Isometric view of the CLD detector (left) ; Vertical cross section showing the top right quadrant of CLD (middle) ; Transverse (XY) cross section of CLD. (right)

4.4 Parametrisation of the reconstructed tracks

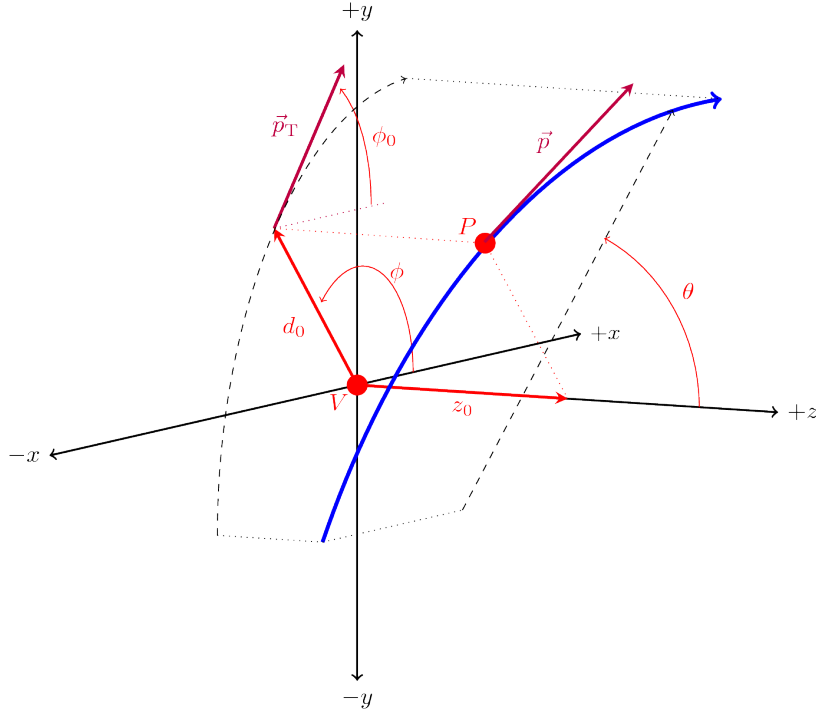


Figure 15: The perigee parametrization of the track helix

We remind that a charged particle has an helix trajectory in the presence of a uniform magnetic field. The interaction of the particle with the tracker layers can lead to the reconstruction of track. This track can be parametrised by 5 parameters and we choose the perigee parametrization [16] illustrated by Figure 15. With this convention, these 5 parameters are measured at the closest point of approach (called perigee and noted P in the figure) of the propeller to the origin of the coordinate system. We give the definition of these parameters:

- the impact parameter d_0 in the transverse plane, *i.e.* the distance in the $x - y$ plane between the perigee and the origin.
- the z -coordinate noted z_0 (and d_z in DELPHES= on the track at the perigee.

- the azimuthal angle ϕ of the track at the perigee.
- the angle θ of the track
- the azimuthal angle ϕ_0 of the transverse momentum.

4.5 Influence of the model parameters on the reconstructed tracks

Due to a lack of time, we did not study the detector sensitivity to signatures relative to long-lived particles. Instead, we had investigated the impact of the HNL life-time and the mass on the reconstructed track parameters. Tables 3 and 4 show the mean values of $|d_0|$ and $|d_z|$ over the reconstructed tracks of the events. Both tables can be interpreted in the same way. Indeed, it is expected that the 3D impact parameter of the tracks corresponding to the HLN daughters increases with the flight distance of the HLN. Besides, we showed in the previous section that the decay width increases with the HNL mass. Therefore, the flight distance of the HLN decreases with its mass. The influence of the HLN $\beta\gamma$ factor can be neglected at first order.

	$m = 10 \text{ GeV}$	$m = 30 \text{ GeV}$	$m = 50 \text{ GeV}$
$c\tau = 1 \text{ cm}$	0.85	0.55	0.29
$c\tau = 10 \text{ cm}$	8.49	5.48	2.90
$c\tau = 100 \text{ cm}$	69.54	52.27	29.03

Table 3: Average of absolute d_0 values, in millimeters, as function of mass and flydistance and 200 generated events

	$m = 10 \text{ GeV}$	$m = 30 \text{ GeV}$	$m = 50 \text{ GeV}$
$c\tau = 1 \text{ cm}$	1.37	0.79	0.42
$c\tau = 10 \text{ cm}$	13.56	7.87	4.21
$c\tau = 100 \text{ cm}$	156.00	92.48	41.25

Table 4: Average of absolute d_z values, in millimeters, as function of mass and flydistance and 200 generated events

Conclusion

This internship addressed a theoretical model which extends the Standard Model and can predict long-lived particle, detectable with the future CLD detector at the FCC-ee.

First, our task was to derive the Lagrangian density of this extension of the Standard Model. We saw that the specific features of the SeeSaw type 1 model, in particular the introduction of a right-handed chiral neutral lepton with a large Majorana mass, can explain the smallness of the standard neutrinos mass. With the help of the mixing between the light and heavy neutrinos, the neutrinos are coupled to the W^\pm , Z^0 and h^0 bosons of the Standard Model. The Feynman rules for these new interaction vertices have been determined. Considering one generation of HLN, the model depends on two parameters: the mixing angle and the HLN mass.

Then, we carried out a phenomenological study of heavy neutrinos. We were interested in the indirect and direct production of the HLN at the FCC-ee and calculated the cross-section. We studied also the decay of the HLN in fermions. The decay widths relative to the different decay channels have been calculated. All the calculations (at leading order) have been done by hand and cross-checked with the software MADGRAPH_AMC@NLO. We highlight the region of the model parameter space for which the HLN have a flight distance between 1 cm and 1 m. Finally, we produced Monte-Carlo sample corresponding to several benchmark points and ran a brief simulation of the CLD detector. We showed the impact of the life-time and the mass of the HLN on the parameters of the reconstructed tracks of CLD such as the d_0 and the d_z .

With more time, we would have focus on other observable like the track multiplicity and have estimated the efficiency of reconstruction. One interesting signature to investigate is the displaced secondary vertices reconstructed with the tracks corresponding to the HLN final states.

Bibliography

- [1] Asli M Abdullahi et al. “The present and future status of heavy neutral leptons”. In: *Journal of Physics G: Nuclear and Particle Physics* 50.2 (Jan. 2023), p. 020501. ISSN: 1361-6471. DOI: [10.1088/1361-6471/ac98f9](https://doi.org/10.1088/1361-6471/ac98f9). URL: <http://dx.doi.org/10.1088/1361-6471/ac98f9>.
- [2] Daniel Alva, Tao Han, and Richard Ruiz. “Heavy Majorana neutrinos from $W\gamma$ fusion at hadron colliders”. In: *Journal of High Energy Physics* 2015.2 (Feb. 2015). ISSN: 1029-8479. DOI: [10.1007/jhep02\(2015\)072](https://doi.org/10.1007/jhep02(2015)072). URL: [http://dx.doi.org/10.1007/JHEP02\(2015\)072](http://dx.doi.org/10.1007/JHEP02(2015)072).
- [3] Stefan Antusch and Oliver Fischer. “Testing sterile neutrino extensions of the Standard Model at future lepton colliders”. In: *Journal of High Energy Physics* 2015.5 (May 2015). ISSN: 1029-8479. DOI: [10.1007/jhep05\(2015\)053](https://doi.org/10.1007/jhep05(2015)053). URL: [http://dx.doi.org/10.1007/JHEP05\(2015\)053](http://dx.doi.org/10.1007/JHEP05(2015)053).
- [4] Jian-Nan Ding, Qin Qin, and Fu-Sheng Yu. “Heavy neutrino searches at future Z-factories”. In: *The European Physical Journal C* 79.9 (2019), p. 766. DOI: [10.1140/epjc/s10052-019-7277-3](https://doi.org/10.1140/epjc/s10052-019-7277-3). URL: <https://doi.org/10.1140/epjc/s10052-019-7277-3>.
- [5] M. Goldhaber, L. Grodzins, and A. W. Sunyar. “Helicity of Neutrinos”. In: *Phys. Rev.* 109 (3 Feb. 1958), pp. 1015–1017. DOI: [10.1103/PhysRev.109.1015](https://link.aps.org/doi/10.1103/PhysRev.109.1015). URL: <https://link.aps.org/doi/10.1103/PhysRev.109.1015>.
- [6] Q. R. Ahmad et al. “Direct Evidence for Neutrino Flavor Transformation from Neutral-Current Interactions in the Sudbury Neutrino Observatory”. In: *Physical Review Letters* 89.1 (June 2002). ISSN: 1079-7114. DOI: [10.1103/physrevlett.89.011301](https://doi.org/10.1103/physrevlett.89.011301). URL: <http://dx.doi.org/10.1103/PhysRevLett.89.011301>.
- [7] Y. Fukuda et al. “Evidence for Oscillation of Atmospheric Neutrinos”. In: *Physical Review Letters* 81.8 (Aug. 1998), pp. 1562–1567. ISSN: 1079-7114. DOI: [10.1103/physrevlett.81.1562](https://doi.org/10.1103/physrevlett.81.1562). URL: <http://dx.doi.org/10.1103/PhysRevLett.81.1562>.
- [8] Steven Weinberg. “Baryon- and Lepton-Nonconserving Processes”. In: *Phys. Rev. Lett.* 43 (21 Nov. 1979), pp. 1566–1570. DOI: [10.1103/PhysRevLett.43.1566](https://link.aps.org/doi/10.1103/PhysRevLett.43.1566). URL: <https://link.aps.org/doi/10.1103/PhysRevLett.43.1566>.
- [9] Richard Ruiz. *The Standard Model + Heavy Neutrinos at NLO in QCD*. URL: <https://feynrules.irmp.ucl.ac.be/wiki/HeavyN>.
- [10] Anupama Atre et al. “The search for heavy Majorana neutrinos”. In: *Journal of High Energy Physics* 2009.05 (May 2009), pp. 030–030. ISSN: 1029-8479. DOI: [10.1088/1126-6708/2009/05/030](https://doi.org/10.1088/1126-6708/2009/05/030). URL: <http://dx.doi.org/10.1088/1126-6708/2009/05/030>.

- [11] A. M. Sirunyan et al. “Search for Heavy Neutral Leptons in Events with Three Charged Leptons in Proton-Proton Collisions at $\sqrt{s} = 13$ TeV”. In: *Phys. Rev. Lett.* 120 (22 May 2018), p. 221801. DOI: [10.1103/PhysRevLett.120.221801](https://doi.org/10.1103/PhysRevLett.120.221801). URL: <https://link.aps.org/doi/10.1103/PhysRevLett.120.221801>.
- [12] J. Alwall et al. “The automated computation of tree-level and next-to-leading order differential cross sections, and their matching to parton shower simulations”. In: *Journal of High Energy Physics* 2014.7 (July 2014). ISSN: 1029-8479. DOI: [10.1007/jhep07\(2014\)079](https://doi.org/10.1007/jhep07(2014)079). URL: [http://dx.doi.org/10.1007/JHEP07\(2014\)079](http://dx.doi.org/10.1007/JHEP07(2014)079).
- [13] Particle Data Group et al. “Review of Particle Physics”. In: *Progress of Theoretical and Experimental Physics* 2022.8 (Aug. 2022), p. 083C01. ISSN: 2050-3911. DOI: [10.1093/ptep/ptac097](https://doi.org/10.1093/ptep/ptac097). eprint: <https://academic.oup.com/ptep/article-pdf/2022/8/083C01/49175539/ptac097.pdf>. URL: <https://doi.org/10.1093/ptep/ptac097>.
- [14] J. de Favereau et al. “DELPHES 3: a modular framework for fast simulation of a generic collider experiment”. In: *Journal of High Energy Physics* 2014.2 (Feb. 2014). ISSN: 1029-8479. DOI: [10.1007/jhep02\(2014\)057](https://doi.org/10.1007/jhep02(2014)057). URL: [http://dx.doi.org/10.1007/JHEP02\(2014\)057](http://dx.doi.org/10.1007/JHEP02(2014)057).
- [15] N. Bacchetta et al. *CLD – A Detector Concept for the FCC-ee*. 2019. arXiv: [1911.12230](https://arxiv.org/abs/1911.12230) [physics.ins-det].
- [16] J. Krohn et al. *Global Decay Chain Vertex Fitting at B-Factories*. Jan. 2019. URL: https://www.researchgate.net/figure/The-perigee-parametrisation-of-the-track-helix-depiction-adapted-from-8-A-description_fig2_330775816.

Appendix A : SM and HNL's Feynman Rules

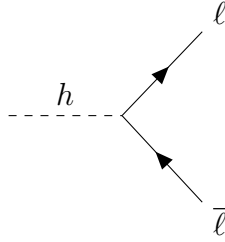
SM Feynman Rules:

Propagators:

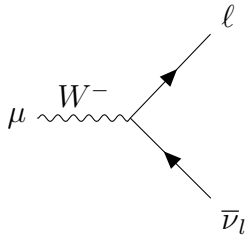
For massive/unstable particle (k) :

$$\frac{-i\eta_{\mu\nu}}{q^2 - m_k^2 + im_k\Gamma_k}$$

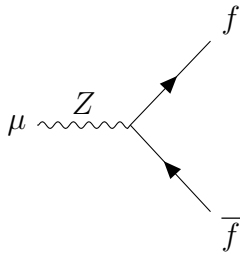
Vertex factors :



$$\frac{-ig_W m_\ell}{2m_W} \quad \text{with} \quad g_W = \frac{e}{\sin \theta_W}$$



$$\frac{-ig_W}{\sqrt{2}} \gamma^\mu P_L \quad \text{with} \quad P_L = \frac{1}{2}(1 - \gamma^5)$$

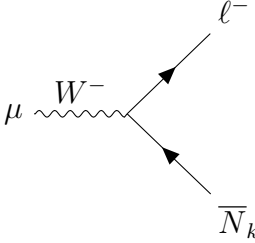
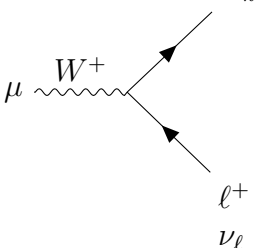
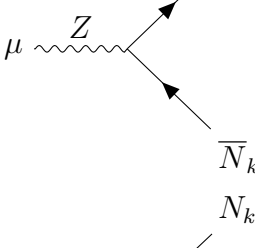
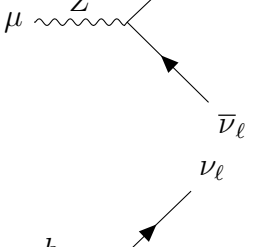
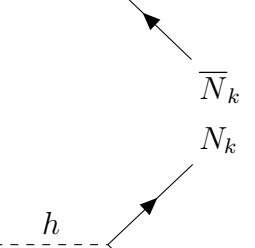
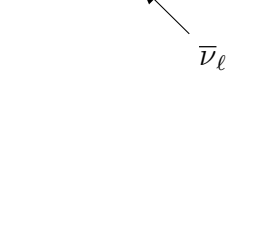


$$\frac{-ig_Z}{2} \gamma^\mu (C_L P_L + C_R P_R) \quad \text{with} \quad g_Z = \frac{e}{\cos \theta_W \sin \theta_W} \quad \text{and} \quad C_L P_L + C_R P_R = (g_V^f - g_A^f \gamma^5)$$

f	g_V^f	g_A^f
ν_ℓ	$\frac{1}{2}$	$\frac{1}{2}$
ℓ	$-\frac{1}{2} + 2 \sin^2 \theta_W$	$-\frac{1}{2}$

HNL's Feynman Rules:

From the interaction term of the Lagrangian density, we can deduce the Feynman rules for those vertex :

	\Longleftrightarrow	$\frac{-ig_W}{\sqrt{2}} V_{\ell k}^* \gamma^\mu P_L$
	\Longleftrightarrow	$\frac{-ig_W}{\sqrt{2}} V_{\ell k} \gamma^\mu P_L$
	\Longleftrightarrow	$\frac{-ig_W}{2 \cos \theta_W} V_{\ell k}^* \gamma^\mu P_L$
	\Longleftrightarrow	$\frac{-ig_W}{2 \cos \theta_W} V_{\ell k} \gamma^\mu P_L$
	\Longleftrightarrow	$\frac{-ig_W m_N}{2M_W} V_{\ell k}^* P_L$
	\Longleftrightarrow	$\frac{-ig_W m_N}{2M_W} V_{\ell k} P_R$

Appendix B : Chirality and helicity projectors

Definition of operators

Chirality operators:

$$P_L = \chi_- = \frac{1}{2} (1 - \gamma^5)$$

$$P_R = \chi_+ = \frac{1}{2} (1 + \gamma^5)$$

Helicity operators:

$$H_-(s) = \frac{1}{2} (1 - \gamma^5 \not{s})$$

$$H_+(s) = \frac{1}{2} (1 + \gamma^5 \not{s})$$

with $s = (\gamma\beta, \gamma\vec{\beta}/\beta)$ and γ^5 the imaginary product of the four Dirac matrices.
Other equivalent definition:

$$H_-(s) = \frac{1}{2} P_R (1 - \not{s}) + \frac{1}{2} P_L (1 + \not{s}) = \frac{1}{2} (1 - \not{s}) P_L + \frac{1}{2} (1 + \not{s}) P_R$$

$$H_+(s) = \frac{1}{2} P_R (1 + \not{s}) + \frac{1}{2} P_L (1 - \not{s}) = \frac{1}{2} (1 + \not{s}) P_L + \frac{1}{2} (1 - \not{s}) P_R$$

$$H(\epsilon, s) = \frac{1}{2} P_R (1 + \epsilon \not{s}) + \frac{1}{2} P_L (1 - \epsilon \not{s}) = \frac{1}{2} (1 + \epsilon \not{s}) P_L + \frac{1}{2} (1 - \epsilon \not{s}) P_R$$

Properties about s

Reminder:

$$E = \gamma m$$

$$p = \beta E$$

$$p = \beta \gamma m$$

$$\text{so } s = \left(\frac{p}{m}, \frac{E}{mp} \vec{p} \right)$$

Useful identities about s :

$$s^2 = -1$$

$$\begin{aligned}
s \cdot p &= \frac{p}{m}E - \frac{E}{mp}\vec{p} \cdot \vec{p} = \frac{p}{m}E - \frac{Ep}{m} = 0 \\
\not{s}^2 &= s^2 \mathbb{1} = -\mathbb{1} \\
\not{s}\not{p} &= -\not{p}\not{s} \\
\not{p}\not{s}\not{p} &= -p^2\not{s}
\end{aligned}$$

Properties of projectors

Coming from the definition of projectors:

$$\begin{aligned}
\chi_- \chi_+ &= \chi_+ \chi_- = 0 \\
\chi_- \chi_- &= \chi_- \\
\chi_+ \chi_+ &= \chi_+ \\
\chi_+ + \chi_- &= \mathbb{1}
\end{aligned}$$

Coming from the definition of projectors:

$$\begin{aligned}
H_-(s)H_+(s) &= H_+(s)H_-(s) = 0 \\
H_-(s)H_-(s) &= H_-(s) \\
H_+(s)H_+(s) &= H_+(s) \\
H_+(s) + H_-(s) &= \mathbb{1}
\end{aligned}$$

Projectors times γ^5 matrix:

$$\begin{aligned}
\gamma^5 \chi_{\pm}(s) &= -\chi_{\pm} \\
\gamma^5 H_{\pm}(s) &= H_{\mp} \gamma^5
\end{aligned}$$

Property with \dagger :

$$\begin{aligned}
\chi_{\pm}^{\dagger} &= \chi_{\pm} \\
H_{\pm}(s)^{\dagger} &= \gamma^0 H_{\pm}(s) \gamma^0
\end{aligned}$$

Dirac adjoint $\bar{}$:

$$\begin{aligned}
\psi_{\pm} = \chi_{\pm} \psi &\rightarrow \bar{\psi}_{\pm} = \bar{\psi} \chi_{\mp} \\
\psi_{\pm} = H_{\pm}(s) \psi &\rightarrow \bar{\psi}_{\pm} = \bar{\psi} H_{\pm}(s)
\end{aligned}$$

Commutation with \not{p} :

$$\not{p} H_{\pm}(s) = H_{\pm}(s) \not{p}$$

Appendix C : Trace identities of Dirac matrices

$$\begin{aligned} & Tr \left[(\not{p}_1 + m_1) \gamma^\mu (\not{p}_2 + m_2) \gamma^\nu \right] \\ &= 4 \left[p_1^\mu p_2^\nu + p_1^\nu p_2^\mu - (p_1 \cdot p_2) \eta^{\mu\nu} + m_1 m_2 \eta^{\mu\nu} \right] \end{aligned}$$

$$\begin{aligned} & Tr \left[(\not{p}_1 + m_1) \gamma^\mu (\not{p}_2 + m_2) \gamma^\nu \chi_\pm \right] \\ &= 2 \left[p_1^\mu p_2^\nu + p_1^\nu p_2^\mu - (p_1 \cdot p_2) \eta^{\mu\nu} + 2m_1 m_2 \eta^{\mu\nu} \pm i p_{1\alpha} p_{2\beta} \epsilon^{\alpha\beta\mu\nu} \right] \end{aligned}$$

$$\begin{aligned} & Tr \left[(\not{p}_1 + m_1) \gamma^\mu (\not{p}_2 + m_2) \gamma^\nu \right] Tr \left[(\not{p}_3 + m_3) \gamma_\mu (\not{p}_4 + m_4) \gamma_\nu \right] \\ &= 32 \left[(p_1 \cdot p_3)(p_2 \cdot p_4) + (p_1 \cdot p_4)(p_3 \cdot p_2) - m_3 m_4 (p_1 \cdot p_2) - m_1 m_2 (p_3 \cdot p_4) + 2m_1 m_2 m_3 m_4 \right] \end{aligned}$$

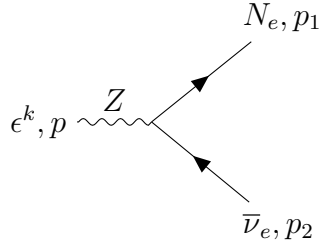
$$\begin{aligned} & Tr \left[(\not{p}_1 + m_1) \gamma^\mu (\not{p}_2 + m_2) \gamma^\nu \right] Tr \left[(\not{p}_3 + m_3) \gamma_\mu (\not{p}_4 + m_4) \gamma_\nu \chi_\pm \right] \\ &= 16 \left[(p_1 \cdot p_3)(p_2 \cdot p_4) + (p_1 \cdot p_4)(p_3 \cdot p_2) - m_3 m_4 (p_1 \cdot p_2) - m_1 m_2 (p_3 \cdot p_4) + 2m_1 m_2 m_3 m_4 \right] \end{aligned}$$

$$\begin{aligned} & Tr \left[(\not{p}_1 + m_1) \gamma^\mu (\not{p}_2 + m_2) \gamma^\nu \chi_\pm \right] Tr \left[(\not{p}_3 + m_3) \gamma_\mu (\not{p}_4 + m_4) \gamma_\nu \chi_\pm \right] \\ &= Tr \left[(\not{p}_1 + m_1) \gamma^\mu (\not{p}_2 + m_2) \gamma^\nu \chi_\pm \right] Tr \left[(\not{p}_3 + m_3) \gamma_\mu (\not{p}_4 + m_4) \gamma_\nu \chi_\mp \right] \\ &= 8 \left[2(p_1 \cdot p_3)(p_2 \cdot p_4) - m_3 m_4 (p_1 \cdot p_2) - m_1 m_2 (p_3 \cdot p_4) + 2m_1 m_2 m_3 m_4 \right] \end{aligned}$$

Appendix D : Full computation of decay-width and cross-sections

Computation of decay rate

$$\Gamma(Z \longrightarrow N_e \bar{\nu}_e)$$



We can compute the matrix element :

$$i\mathcal{M} = \epsilon_\mu^k \left[\bar{u}_1 \left(\frac{-ig_Z}{2} V_{\ell k} \gamma^\mu P_L \right) v_2 \right]$$

and

$$-i\mathcal{M}^\dagger = \epsilon_\nu^{*k} \left[\bar{v}_2 \left(\frac{ig_Z}{2} V_{\ell k}^* \gamma^\nu P_L \right) u_1 \right]$$

Then we have :

$$|\mathcal{M}|^2 = \frac{g_Z^2 |V_{\ell k}|^2}{4} \epsilon_\mu^k \epsilon_\nu^{*k} \left[\bar{u}_1 \gamma^\mu P_L v_2 \right] \left[\bar{v}_2 \gamma^\nu P_L u_1 \right]$$

There are 3 possible polarisation states, so we average over initial state and we sum over final state:

$$|\overline{\mathcal{M}}|^2 = \frac{1}{3} \sum_k \epsilon_\mu^k \epsilon_\nu^{*k} \frac{g_Z^2 |V_{\ell k}|^2}{4} \sum_{1,2} \left[\bar{u}_1 \gamma^\mu P_L v_2 \right] \left[\bar{v}_2 \gamma^\nu P_L u_1 \right]$$

and we have the following identity :

$$\sum_k \epsilon_\mu^k(p) \epsilon_\nu^{*k}(p) = -\eta_{\mu\nu} + \frac{p_\mu p_\nu}{m_Z^2}$$

So we can replace

$$\begin{aligned} |\overline{\mathcal{M}}|^2 &= \frac{g_Z^2 |V_{\ell k}|^2}{12} \left(-\eta_{\mu\nu} + \frac{p_\mu p_\nu}{m_Z^2} \right) \sum_{1,2} \left[\bar{u}_1 \gamma^\mu P_L v_2 \right] \left[\bar{v}_2 \gamma^\nu P_L u_1 \right] \\ &= \frac{g_Z^2 |V_{\ell k}|^2}{12} \left(-\eta_{\mu\nu} + \frac{p_\mu p_\nu}{m_Z^2} \right) \text{Tr} \left((\not{p}_1 + m_1) \gamma^\mu \not{p}_2 \gamma^\nu P_L \right) \end{aligned}$$

The trace identity is :

$$\begin{aligned} & Tr\left((\not{p}_1 + m_1)\gamma^\mu(\not{p}_2 + m_2)\gamma^\nu P_{R/L}\right) \\ &= 2\left[p_1^\mu p_2^\nu + p_1^\nu p_2^\mu - (p_1 \cdot p_2)\eta^{\mu\nu} + 2m_1 m_2 \eta^{\mu\nu} \pm i p_{1\alpha} p_{2\beta} \epsilon^{\alpha\beta\mu\nu}\right] \end{aligned}$$

So here we have

$$\begin{aligned} |\overline{\mathcal{M}}|^2 &= \frac{g_Z^2 |V_{\ell k}|^2}{6} \left(-\eta_{\mu\nu} + \frac{p_\mu p_\nu}{m_Z^2}\right) \left[p_1^\mu p_2^\nu + p_1^\nu p_2^\mu - (p_1 \cdot p_2)\eta^{\mu\nu}\right] \\ &= \frac{g_Z^2 |V_{\ell k}|^2}{6} \left[2p_1 \cdot p_2 + \frac{2(p_1 \cdot p)(p_2 \cdot p)}{m_Z^2} - \frac{(p_1 \cdot p_2)p^2}{m_Z^2}\right] \end{aligned}$$

and we have :

$$\begin{aligned} p_1 &= \left(\frac{s + m_1^2}{2\sqrt{s}}, \frac{s - m_1^2}{2\sqrt{s}} \vec{v}\right) \\ p_2 &= \left(\frac{s - m_1^2}{2\sqrt{s}}, -\frac{s - m_1^2}{2\sqrt{s}} \vec{v}\right) \\ p &= p_1 + p_2 = (\sqrt{s}, 0) = (m_Z, 0) \end{aligned}$$

So :

$$\begin{aligned} p_1 \cdot p_2 &= \frac{s + m_1^2}{2\sqrt{s}} \frac{s - m_1^2}{2\sqrt{s}} + \frac{s - m_1^2}{2\sqrt{s}} \frac{s - m_1^2}{2\sqrt{s}} \\ &= \frac{s^2 - m_1^4}{4s} + \frac{s^2 + m_1^4 - 2sm_1^2}{4s} \\ &= \frac{s}{2} \left(1 - \frac{m_1^2}{s}\right) \end{aligned}$$

and

$$\frac{2}{m_Z^2} (p_1 \cdot p)(p_2 \cdot p) = \frac{m_Z^2}{2} \left(1 - \frac{m_1^4}{m_Z^4}\right)$$

So finally :

$$|\overline{\mathcal{M}}|^2 = \frac{g_Z^2 |V_{\ell k}|^2 m_Z^2}{12} \left(\left(1 - \frac{m_1^2}{m_Z^2}\right) + \left(1 - \frac{m_1^4}{m_Z^4}\right) \right)$$

The decay width formula adapted for 1×2 processes in center-of-mass frame is :

$$\frac{d\Gamma^*}{d\Omega^*} = \frac{1}{64\pi^2 M^3} \sqrt{\lambda(M^2, m_1^2, m_2^2)} |\overline{\mathcal{M}}|^2$$

where M is the mass of the incoming particle, and λ the Källén function. In our case, we have :

$$\begin{aligned} \frac{d\Gamma^*}{d\Omega^*} &= \frac{1}{64\pi^2 m_Z^3} \sqrt{m_Z^4 + m_1^4 - 2m_Z^2 m_1^2} |\overline{\mathcal{M}}|^2 \\ &= \frac{1 - \frac{m_1^2}{m_Z^2}}{64\pi^2 m_Z} \frac{g_Z^2 |V_{\ell k}|^2 m_Z^2}{12} \left(\left(1 - \frac{m_1^2}{m_Z^2}\right) + \left(1 - \frac{m_1^4}{m_Z^4}\right) \right) \end{aligned}$$

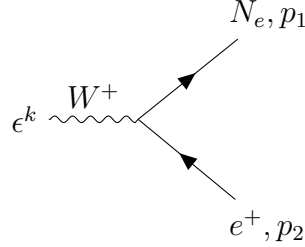
And to obtain the integrated decay width

$$\begin{aligned}\Gamma &= \int_{\phi=0}^{2\pi} \int_{\cos\theta=-1}^1 \frac{d\Gamma^*}{d\Omega^*} d\cos\theta d\phi \\ &= 4\pi \frac{d\Gamma^*}{d\Omega^*}\end{aligned}$$

And in our case s is m_Z^2 so we obtain the following partial width :

$$\Gamma(Z \longrightarrow N_e \bar{\nu}_e) = \frac{g_Z^2 |V_{\ell k}|^2 m_Z}{192 \pi} \left(\left(1 - \frac{m^2}{m_Z^2}\right)^2 + \left(1 - \frac{m^2}{m_Z^2}\right) \left(1 - \frac{m^4}{m_Z^4}\right) \right)$$

$$\Gamma(W \longrightarrow N_e e^+)$$



We can compute the matrix element :

$$i\mathcal{M} = \epsilon_\mu^k \left[\bar{u}_1 \left(\frac{-ig_W}{\sqrt{2}} V_{\ell k} \gamma^\mu P_L \right) v_2 \right]$$

and

$$-i\mathcal{M}^\dagger = \epsilon_\nu^{*k} \left[\bar{v}_2 \left(\frac{ig_W}{2} V_{\ell k}^* \gamma^\nu P_L \right) u_1 \right]$$

Then we have :

$$|\mathcal{M}|^2 = \frac{g_W^2 |V_{\ell k}|^2}{2} \epsilon_\mu^k \epsilon_\nu^{*k} \left[\bar{u}_1 \gamma^\mu P_L v_2 \right] \left[\bar{v}_2 \gamma^\nu P_L u_1 \right]$$

$$|\overline{\mathcal{M}}|^2 = \frac{1}{3} \sum_k \epsilon_\mu^k \epsilon_\nu^{*k} \frac{g_W^2 |V_{\ell k}|^2}{2} \sum_{1,2} \left[\bar{u}_1 \gamma^\mu P_L v_2 \right] \left[\bar{v}_2 \gamma^\nu P_L u_1 \right]$$

and we have the following identity :

$$\sum_k \epsilon_\mu^k(p) \epsilon_\nu^{*k}(p) = -\eta_{\mu\nu} + \frac{p_\mu p_\nu}{m_W^2}$$

So we can replace

$$\begin{aligned}|\overline{\mathcal{M}}|^2 &= \frac{g_Z^2 |V_{\ell k}|^2}{6} \left(-\eta_{\mu\nu} + \frac{p_\mu p_\nu}{m_W^2} \right) \sum_{1,2} \left[\bar{u}_1 \gamma^\mu P_L v_2 \right] \left[\bar{v}_2 \gamma^\nu P_L u_1 \right] \\ &= \frac{g_Z^2 |V_{\ell k}|^2}{6} \left(-\eta_{\mu\nu} + \frac{p_\mu p_\nu}{m_W^2} \right) \text{Tr} \left((\not{p}_1 + m_1) \gamma^\mu \not{p}_2 \gamma^\nu P_L \right)\end{aligned}$$

The trace identity is :

$$\begin{aligned} & Tr \left((\not{p}_1 + m_1) \gamma^\mu (\not{p}_2 + m_2) \gamma^\nu P_{R/L} \right) \\ &= 2 \left[p_1^\mu p_2^\nu + p_1^\nu p_2^\mu - (p_1 \cdot p_2) \eta^{\mu\nu} + 2m_1 m_2 \eta^{\mu\nu} \pm i p_{1\alpha} p_{2\beta} \epsilon^{\alpha\beta\mu\nu} \right] \end{aligned}$$

So here we have

$$\begin{aligned} |\overline{\mathcal{M}}|^2 &= \frac{g_W^2 |V_{\ell k}|^2}{3} \left(-\eta_{\mu\nu} + \frac{p_\mu p_\nu}{m_W^2} \right) \left[p_1^\mu p_2^\nu + p_1^\nu p_2^\mu - (p_1 \cdot p_2) \eta^{\mu\nu} \right] \\ &= \frac{g_W^2 |V_{\ell k}|^2}{3} \left[2p_1 \cdot p_2 + \frac{2(p_1 \cdot p)(p_2 \cdot p)}{m_W^2} - \frac{(p_1 \cdot p_2)p^2}{m_W^2} \right] \\ &= \frac{g_W^2 |V_{\ell k}|^2 m_W^2}{4} \left(\left(1 - \frac{m^2}{m_W^2} \right) + \left(1 - \frac{m^4}{m_W^4} \right) \right) \end{aligned}$$

The decay width formula adapted for 1×2 processes in center-of-mass frame is :

$$\frac{d\Gamma^*}{d\Omega^*} = \frac{1}{64\pi^2 M^3} \sqrt{\lambda(M^2, m_1^2, m_2^2)} |\overline{\mathcal{M}}|^2$$

where M is the mass of the incoming particle, and λ the Källén function. In our case, we have :

$$\begin{aligned} \frac{d\Gamma^*}{d\Omega^*} &= \frac{1}{64\pi^2 m_W^3} \sqrt{m_W^4 + m_1^4 - 2m_W^2 m_1^2} |\overline{\mathcal{M}}|^2 \\ &= \frac{1 - \frac{m_1^2}{m_W^2}}{64\pi^2 m_W} \frac{g_W^2 |V_{\ell k}|^2 m_W^2}{6} \left(\left(1 - \frac{m^2}{m_W^2} \right) + \left(1 - \frac{m^4}{m_W^4} \right) \right) \end{aligned}$$

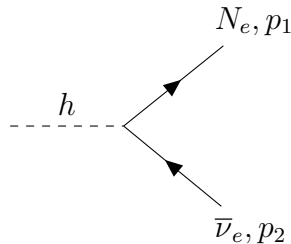
And to obtain the integrated decay width

$$\begin{aligned} \Gamma &= \int_{\phi=0}^{2\pi} \int_{\cos \theta=-1}^1 \frac{d\Gamma^*}{d\Omega^*} d\cos \theta d\phi \\ &= 4\pi \frac{d\Gamma^*}{d\Omega^*} \end{aligned}$$

And in our case s is m_W^2 so we obtain the following partial width :

$$\Gamma(W^+ \longrightarrow N_e e^+) = \frac{g_W^2 |V_{\ell k}|^2 m_W}{92\pi} \left(\left(1 - \frac{m^2}{m_W^2} \right)^2 + \left(1 - \frac{m^2}{m_W^2} \right) \left(1 - \frac{m^4}{m_W^4} \right) \right)$$

$$\Gamma(h \longrightarrow N_e \bar{\nu}_e)$$



We can compute the matrix element :

$$i\mathcal{M} = \left[\bar{u}_1 \left(\frac{-ig_W m_1}{2m_W} V_{\ell k} P_R \right) v_2 \right]$$

and

$$-i\mathcal{M}^\dagger = \left[\bar{v}_2 \left(\frac{ig_W m_1}{2m_W} V_{\ell k}^* P_L \right) u_1 \right]$$

Then we have :

$$\begin{aligned} |\mathcal{M}|^2 &= \frac{g_W^2 |V_{\ell k}|^2 m_1^2}{4m_W^2} \left[\bar{u}_1 P_R v_2 \right] \left[\bar{v}_2 P_L u_1 \right] \\ |\overline{\mathcal{M}}|^2 &= \frac{g_W^2 |V_{\ell k}|^2 m_1^2}{4m_W^2} \sum_{1,2} \left[\bar{u}_1 P_R v_2 \right] \left[\bar{v}_2 P_L u_1 \right] \\ &= \frac{g_W^2 |V_{\ell k}|^2 m_1^2}{4m_W^2} \text{Tr} \left((p_1 + m_1) \not{p}_2 P_L \right) \\ &= \frac{g_W^2 |V_{\ell k}|^2 m_1^2}{8m_W^2} p_1^\mu p_2^\nu \text{Tr} \left(\gamma_\mu \gamma_\nu \right) \\ &= \frac{g_W^2 |V_{\ell k}|^2 m_1^2}{8m_W^2} p_1^\mu p_2^\nu 4\eta_{\mu\nu} \\ &= \frac{g_W^2 |V_{\ell k}|^2 m_1^2}{2m_W^2} (p_1 \cdot p_2) \\ &= \frac{g_W^2 |V_{\ell k}|^2}{4m_W^2} s \left(1 - \frac{m^2}{s} \right) m_1^2 \end{aligned}$$

The decay width formula adapted for 1×2 processes in center-of-mass frame is :

$$\frac{d\Gamma^*}{d\Omega^*} = \frac{1}{64\pi^2 M^3} \sqrt{\lambda(M^2, m_1^2, m_2^2)} |\overline{\mathcal{M}}|^2$$

where M is the mass of the incoming particle, and λ the Källén function. In our case, we have :

$$\begin{aligned} \frac{d\Gamma^*}{d\Omega^*} &= \frac{1}{64\pi^2 m_h^3} \sqrt{m_h^4 + m_1^4 - 2m_h^2 m_1^2} |\overline{\mathcal{M}}|^2 \\ &= \frac{|m_h^2 - m_1^2|}{64\pi^2 m_h^3} \frac{g_W^2 |V_{\ell k}|^2}{4m_W^2} s \left(1 - \frac{m^2}{s} \right) m_1^2 \end{aligned}$$

And to obtain the integrated decay width

$$\begin{aligned} \Gamma &= \int_{\phi=0}^{2\pi} \int_{\cos\theta=-1}^1 \frac{d\Gamma^*}{d\Omega^*} d\cos\theta d\phi \\ &= 4\pi \frac{d\Gamma^*}{d\Omega^*} \end{aligned}$$

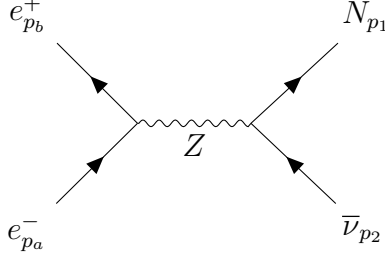
And in our case s is m_h^2 so we obtain the following partial width :

$$\Gamma(h \longrightarrow N_e \bar{\nu}_e) = \frac{g_W^2 |V_{\ell k}|^2}{64\pi m_W^2} m_N^2 m_h \left(1 - \frac{m_N^2}{m_h^2} \right)^2$$

Process $e^+ e^- \longrightarrow Z \longrightarrow \bar{\nu}_e N_1$

Calculation of the matrix element

We want to compute the cross section of this process :



In the following we will note $g_Z = \frac{g_W}{\cos \theta_W}$ with $g_W = \frac{e}{\sin \theta_W}$ the gauge coupling for $SU(2)_L$, and $C_L P_L + C_R P_R$ instead of $g_V - g_A \gamma^5$

Start by calculating $i\mathcal{M}$:

$$i\mathcal{M} = \left[\bar{v}_b \left(\frac{-ig_W}{2 \cos \theta_W} \gamma^\mu (C_L P_L + C_R P_R) \right) u_a \right] \left[\frac{-i\eta_{\mu\nu}}{q^2 - m_Z^2 + im_Z \Gamma_Z} \right] \left[\bar{u}_1 \left(\frac{-ig_W}{2 \cos \theta_W} V_{\ell k} \gamma^\nu P_L \right) v_2 \right]$$

$$i\mathcal{M} = \frac{ig_Z^2 V_{\ell k}}{4(s - m_Z^2 + im_Z \Gamma_Z)} \left[\bar{v}_b \gamma^\mu (C_L P_L + C_R P_R) u_a \right] \left[\bar{u}_1 \gamma_\mu P_L v_2 \right]$$

Then we calculate $i\mathcal{M}^\dagger$:

$$\begin{aligned} -i\mathcal{M}^\dagger &= \frac{-ig_Z^2 V_{\ell k}}{4(s - m_Z^2 - im_Z \Gamma_Z)} \left[\bar{u}_1 \gamma_\mu P_L v_2 \right]^\dagger \left[\bar{v}_b \gamma^\mu (C_L P_L + C_R P_R) u_a \right]^\dagger \\ &= \frac{-ig_Z^2 V_{\ell k}}{4(s - m_Z^2 - im_Z \Gamma_Z)} \left[v_2^\dagger P_L (\gamma^0 \gamma_\nu \gamma^0) \bar{u}_1^\dagger \right] \left[u_a^\dagger (C_L P_L + C_R P_R) (\gamma^0 \gamma^\nu \gamma^0) \bar{v}_b^\dagger \right] \\ &= \frac{-ig_Z^2 V_{\ell k}}{4(s - m_Z^2 - im_Z \Gamma_Z)} \left[\bar{v}_2 \gamma_\nu P_L u_1 \right] \left[\bar{u}_a \gamma^\nu (C_L P_L + C_R P_R) v_b \right] \end{aligned}$$

We can then calculate $|\mathcal{M}|^2$

$$|\mathcal{M}|^2 = \frac{g_Z^4 (V_{\ell k})^2}{16((s - m_Z^2)^2 + (m_Z \Gamma_Z)^2)} \left[\bar{v}_b \gamma^\mu (C_L P_L + C_R P_R) u_a \right] \left[\bar{u}_1 \gamma_\mu P_L v_2 \right] \left[\bar{v}_2 \gamma_\nu P_L u_1 \right] \left[\bar{u}_a \gamma^\nu (C_L P_L + C_R P_R) v_b \right]$$

We now calculate $|\overline{\mathcal{M}}|^2$, we average over initial state and we sum over final state:

$$\begin{aligned}
|\overline{\mathcal{M}}|^2 &= \sum_{s_1, s_2} \times \frac{1}{2} \sum_{s_a} \times \frac{1}{2} \sum_{s_b} |\mathcal{M}|^2 \\
&= \frac{g_Z^4 (V_{\ell k})^2}{64 \left((s - m_Z^2)^2 + (m_Z \Gamma_Z)^2 \right)} \sum_{s_1, s_2} \left[\overline{u}_1 \gamma_\mu P_L v_2 \right] \left[\overline{v}_2 \gamma_\nu P_L u_1 \right] \\
&\times \sum_{s_a, s_b} \left[\overline{v}_b \gamma^\mu (C_L P_L + C_R P_R) u_a \right] \left[\overline{u}_a \gamma^\nu (C_L P_L + C_R P_R) v_b \right] \\
&= \frac{g_Z^4 (V_{\ell k})^2}{64 \left((s - m_Z^2)^2 + (m_Z \Gamma_Z)^2 \right)} \text{Tr} \left((\not{p}_1 + m_1) \gamma_\mu P_L (\not{p}_2 - m_2) \gamma_\nu P_L \right) \\
&\text{Tr} \left((\not{p}_a + m_a) \gamma^\mu (C_L P_L + C_R P_R) (\not{p}_b - m_b) \gamma^\nu (C_L P_L + C_R P_R) \right)
\end{aligned}$$

We can neglect the masses m_2 , m_a and m_b and group the P_L and P_R together :

$$|\overline{\mathcal{M}}|^2 = \frac{g_Z^4 (V_{\ell k})^2}{64 \left((s - m_Z^2)^2 + (m_Z \Gamma_Z)^2 \right)} \text{Tr} \left(\not{p}_1 \gamma_\mu \not{p}_2 \gamma_\nu P_L \right) \text{Tr} \left(\not{p}_a \gamma^\mu \not{p}_b \gamma^\nu (C_L^2 P_L + C_R^2 P_R) \right)$$

We have the following trace identity :

$$\begin{aligned}
&\text{Tr} \left(\not{p}_1 \gamma_\mu \not{p}_2 \gamma_\nu P_L \right) \text{Tr} \left(\not{p}_a \gamma^\mu \not{p}_b \gamma^\nu P_L \right) \\
&= \text{Tr} \left(\not{p}_1 \gamma_\mu \not{p}_2 \gamma_\nu P_L \right) \text{Tr} \left(\not{p}_a \gamma^\mu \not{p}_b \gamma^\nu P_R \right) \\
&= 16 (p_1 \cdot p_a) (p_2 \cdot p_b)
\end{aligned}$$

This gives :

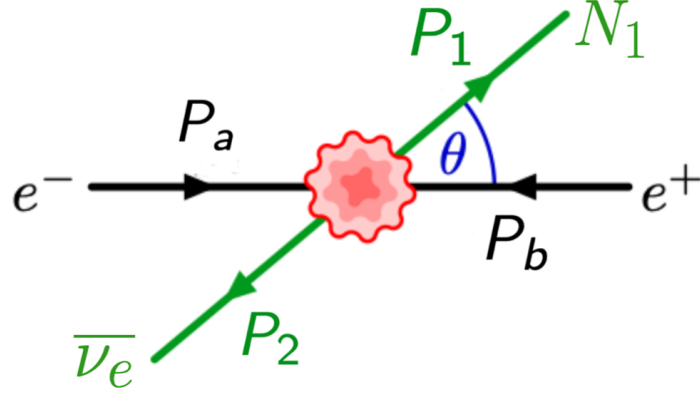
$$|\overline{\mathcal{M}}|^2 = \frac{g_Z^4 (V_{\ell k})^2 (C_L^2 + C_R^2)}{4 \left((s - m_Z^2)^2 + (m_Z \Gamma_Z)^2 \right)} (p_1 \cdot p_a) (p_2 \cdot p_b)$$

Mandelstam's variables are defined as follows:

$$\begin{aligned}
t &= (p_a - p_1)^2 \approx m_1^2 - 2p_a \cdot p_1 \implies p_a \cdot p_1 = -\frac{t - m_1^2}{2} \\
t &= (p_b - p_2)^2 \approx -2p_b \cdot p_2 \implies p_b \cdot p_2 = -\frac{t}{2}
\end{aligned}$$

This gives :

$$|\overline{\mathcal{M}}|^2 = \frac{g_Z^4 (V_{\ell k})^2 (C_L^2 + C_R^2)}{16 \left((s - m_Z^2)^2 + (m_Z \Gamma_Z)^2 \right)} (t^2 - t m_1^2)$$



kinematic calculation :

We define θ as the angle between p_a and p_1 , or between \vec{u} and \vec{v} where u and v are the unit vectors associated with p_a and p_1 respectively. Thus we can write the 4-vectors :

$$\begin{aligned}
 p_a &= \left(\frac{\sqrt{s}}{2}, \frac{\sqrt{s}}{2} \vec{u} \right) \\
 p_b &= \left(\frac{\sqrt{s}}{2}, -\frac{\sqrt{s}}{2} \vec{u} \right) \\
 p_1 &= \left(\frac{s + m_1^2}{2\sqrt{s}}, \frac{s - m_1^2}{2\sqrt{s}} \vec{v} \right) \\
 p_2 &= \left(\frac{s - m_1^2}{2\sqrt{s}}, -\frac{s - m_1^2}{2\sqrt{s}} \vec{v} \right)
 \end{aligned}$$

The formula for the differential cross-section for a reaction 2×2 in the reference frame of the centre of mass is

$$\frac{d\sigma^*}{d\Omega^*} = \frac{1}{64\pi^2 s} \frac{|\vec{p}'|}{|\vec{p}|} |\overline{\mathcal{M}}|^2$$

Here we have (according to the Källén function) :

$$\frac{|\vec{p}'|}{|\vec{p}|} = \left(1 - \frac{m_1^2}{s} \right)$$

and

$$|\overline{\mathcal{M}}|^2 = \frac{g_Z^4 V_{\ell k}^2 (C_L^2 + C_R^2)}{16 \left((s - m_Z^2)^2 + (m_Z \Gamma_Z)^2 \right)} (t^2 - t m_1^2)$$

with t :

$$\begin{aligned}
t &= (p_a - p_1)^2 \\
&= m_1^2 - 2p_a p_1 \\
&= m_1^2 - 2 \left(\frac{\sqrt{s}}{2} \frac{s + m_1^2}{2\sqrt{s}} - \frac{\sqrt{s}}{2} \frac{s - m_1^2}{2\sqrt{s}} \cos \theta \right) \\
&= m_1^2 - \frac{1}{2} \left(s + m_1^2 - (s - m_1^2) \cos \theta \right) \\
&= \frac{m_1^2 - s}{2} (1 - \cos \theta)
\end{aligned}$$

and we have also :

$$t^2 = \left(\frac{m_1^2 - s}{2} \right)^2 (1 - \cos \theta)^2$$

We can therefore replace in the expression of $|\overline{\mathcal{M}}|^2$:

$$|\overline{\mathcal{M}}|^2 = \frac{g_Z^4 (V_{\ell k})^2 (C_L^2 + C_R^2)}{16 \left((s - m_Z^2)^2 + (m_Z \Gamma_Z)^2 \right)} \left(\left(\frac{m_1^2 - s}{2} \right)^2 (1 - \cos \theta)^2 - m_1^2 \frac{m_1^2 - s}{2} (1 - \cos \theta) \right)$$

We can now compute the differential cross section :

$$\begin{aligned}
\frac{d\sigma^*}{d\Omega^*} &= \frac{1}{64\pi^2 s} \left(1 - \frac{m_1^2}{s} \right) |\overline{\mathcal{M}}|^2 \\
&= \frac{g_Z^4 (V_{\ell k})^2 (C_L^2 + C_R^2)}{1024\pi^2 \left((s - m_Z^2)^2 + (m_Z \Gamma_Z)^2 \right)} \frac{1}{s} \left(1 - \frac{m_1^2}{s} \right) \left(\left(\frac{m_1^2 - s}{2} \right)^2 (1 - \cos \theta)^2 - m_1^2 \frac{m_1^2 - s}{2} (1 - \cos \theta) \right)
\end{aligned}$$

We integrate to obtain the effective cross-section :

$$\begin{aligned}
\sigma &= \int_{\phi=0}^{2\pi} \int_{\cos \theta=-1}^1 \frac{d\sigma^*}{d\Omega^*} d\cos \theta d\phi \\
&= \frac{g_Z^4 (V_{\ell k})^2 (C_L^2 + C_R^2)}{1024\pi^2 \left((s - m_Z^2)^2 + (m_Z \Gamma_Z)^2 \right)} \frac{1}{s} \left(1 - \frac{m_1^2}{s} \right) \left(\left(\frac{m_1^2 - s}{2} \right)^2 2\pi \frac{8}{3} - m_1^2 \frac{m_1^2 - s}{2} 4\pi \right) \\
&= \frac{g_Z^4 (V_{\ell k})^2 (C_L^2 + C_R^2)}{512\pi \left((s - m_Z^2)^2 + (m_Z \Gamma_Z)^2 \right)} \frac{1}{s} \left(1 - \frac{m_1^2}{s} \right) \left(\frac{2}{3} (m_1^2 - s)^2 - m_1^2 (m_1^2 - s) \right)
\end{aligned}$$

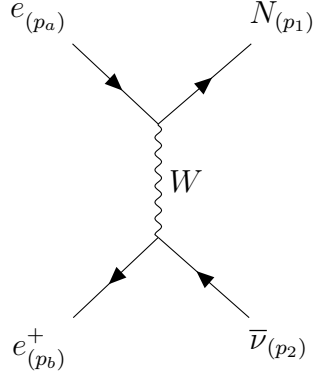
In the end, we have :

$$\sigma_Z = \frac{g_Z^4 (V_{\ell k})^2 (C_L^2 + C_R^2) s}{1536\pi \left((s - m_Z^2)^2 + (m_Z \Gamma_Z)^2 \right)} (r^2 + 2)(1 - r^2)^2$$

with $r = m_1/\sqrt{s} \in [0; 1]$. σ is expressed in GeV^{-2} ; To convert to barn, we have the following relationship : $1 \text{ GeV}^{-2} = 0.3894 \text{ mb}$

Process $e^+ e^- \longrightarrow W \longrightarrow \bar{\nu}_e N_1$

Calculation of the matrix element



$$i\mathcal{M} = \left[\bar{u}_1 \left(\frac{-ig_W}{\sqrt{2}} V_{\ell k} \gamma^\mu P_L \right) u_a \right] \left[\frac{-i\eta_{\mu\nu}}{q^2 - m_W^2 + im_W \Gamma_W} \right] \left[\bar{v}_b \left(\frac{-ig_W}{\sqrt{2}} \gamma^\nu P_L \right) v_2 \right]$$

$$i\mathcal{M} = \frac{ig_W^2 V_{\ell k}}{2(t - m_W^2 + im_W \Gamma_W)} \left[\bar{u}_1 \gamma^\mu P_L u_a \right] \left[\bar{v}_b \gamma_\mu P_L v_2 \right]$$

$$-i\mathcal{M}^\dagger = \frac{-ig_W^2 V_{\ell k}}{2(t - m_W^2 - im_W \Gamma_W)} \left[\bar{v}_2 \gamma_\nu P_L v_b \right] \left[\bar{u}_a \gamma^\nu P_L u_1 \right]$$

We can then calculate $|\mathcal{M}|^2$ and then $|\overline{\mathcal{M}}|^2$:

$$|\mathcal{M}|^2 = \frac{g_W^4 V_{\ell k}^2}{4\left((t - m_W^2)^2 + (m_W \Gamma_W)^2\right)} \left[\bar{u}_1 \gamma^\mu P_L u_a \right] \left[\bar{v}_b \gamma_\mu P_L v_2 \right] \left[\bar{v}_2 \gamma_\nu P_L v_b \right] \left[\bar{u}_a \gamma^\nu P_L u_1 \right]$$

$$|\overline{\mathcal{M}}|^2 = \frac{g_W^4 V_{\ell k}^2}{16\left((t - m_W^2)^2 + (m_W \Gamma_W)^2\right)} \text{Tr} \left(\not{p}_a \gamma_\mu \not{p}_1 \gamma_\nu P_L \right) \text{Tr} \left(\not{p}_2 \gamma_\mu \not{p}_b \gamma_\nu P_L \right)$$

$$= \frac{g_W^4 V_{\ell k}^2}{\left((t - m_W^2)^2 + (m_W \Gamma_W)^2\right)} (p_a p_2)(p_1 p_b)$$

$$= -\frac{g_W^4 V_{\ell k}^2}{4\left((t - m_W^2)^2 + (m_W \Gamma_W)^2\right)} u(m_1^2 - u)$$

With kinematic study, we get Mandelstam variables and the cross section is (we take $x = \cos \theta$):

$$t = \frac{m_1^2 - s}{2}(1 - \cos \theta) \quad \text{and} \quad u = \frac{m_1^2 - s}{2}(1 + \cos \theta)$$

$$\sigma = -\frac{g_W^4 V_{\ell k}^2}{128\pi s} \left(1 - \frac{m_1^2}{s}\right) \int_{x=-1}^1 \frac{m_1^2 \frac{m_1^2-s}{2} (1+x) - \left(\frac{m_1^2-s}{2}\right)^2 (1+x)^2}{\left(\frac{m_1^2-s}{2} (1-x) - m_W^2\right)^2 + (m_W \Gamma_W)^2} dx$$

$$\sigma = \frac{g_W^4 V_{\ell k}^2}{128\pi s} (1-r^2)^2 \int_{x=-1}^1 \frac{(1+x)[(r^2+1) + (1-r^2)x]}{\left((1-r^2)(x-1) - 2r_W^2\right)^2 + 4r_W^2 \gamma_W^2} dx$$

with $r = \frac{m}{\sqrt{s}}$, $r_W = \frac{m_W}{\sqrt{s}}$ and $\gamma_W = \frac{\Gamma_W}{\sqrt{s}}$.

$$\sigma = \frac{g_W^4 V_{\ell k}^2}{128\pi s} (1-r^2)^2 \int_{x=-1}^1 \frac{(1-r^2)x^2 + 2x + (r^2+1)}{(1-r^2)^2 x^2 - 2x(1-r^2)((1-r^2) + 2r_W^2) + ((1-r^2) + 2r_W^2)^2 + 4r_W^2 \gamma_W^2} dx$$

Working with the rational fraction:

$$\begin{aligned} & (1-r^2) \cdot \frac{(1-r^2)x^2 + 2x + (r^2+1)}{(1-r^2)^2 x^2 - 2x(1-r^2)((1-r^2) + 2r_W^2) + ((1-r^2) + 2r_W^2)^2 + 4r_W^2 \gamma_W^2} \\ &= 1 + \frac{2(1-r^2)(2-r^2+2r_W^2)x + (1-r^4) - ((1-r^2) + 2r_W^2)^2 - 4r_W^2 \gamma_W^2}{\left((1-r^2)(x-1) - 2r_W^2\right)^2 + 4r_W^2 \gamma_W^2} \\ &= 1 + \frac{2-r^2+2r_W^2}{1-r^2} \frac{2(1-r^2)^2 x - 2(1-r^2)((1-r^2) + 2r_W^2)}{\left((1-r^2)(x-1) - 2r_W^2\right)^2 + 4r_W^2 \gamma_W^2} \\ &\quad + \frac{2-r^2+2r_W^2}{1-r^2} \frac{2(1-r^2)((1-r^2) + 2r_W^2)}{\left((1-r^2)(x-1) - 2r_W^2\right)^2 + 4r_W^2 \gamma_W^2} \\ &\quad + \frac{(1-r^4) - ((1-r^2) + 2r_W^2)^2 - 4r_W^2 \gamma_W^2}{\left((1-r^2)(x-1) - 2r_W^2\right)^2 + 4r_W^2 \gamma_W^2} \end{aligned}$$

Integral:

$$\sigma = \frac{g_W^4 V_{\ell k}^2}{128\pi s} (1-r^2)(I_1 + I_2 + I_3)$$

with:

$$I_1 = \int_{-1}^{+1} 1 dx = 2$$

$$I_2 = \frac{2-r^2+2r_W^2}{1-r^2} \left[\log \left(\left((1-r^2)(x-1) - 2r_W^2 \right)^2 + 4r_W^2 \gamma_W^2 \right) \right]_{-1}^{+1}$$

$$I_2 = \frac{2-r^2+2r_W^2}{1-r^2} \log \left(\frac{r_W^2(r_W^2 + \gamma_W^2)}{((1-r^2) + r_W^2)^2 + r_W^2 \gamma_W^2} \right)$$

$$I_3 = K \int_{-1}^{+1} dx \frac{1}{\left((1-r^2)(x-1) - 2r_W^2\right)^2 + 4r_W^2 \gamma_W^2}$$

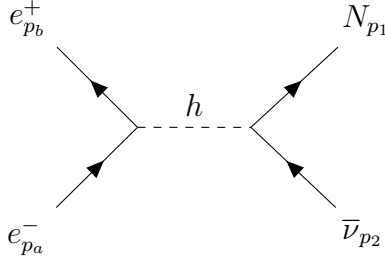
$$\begin{aligned}
I_3 &= K \frac{1}{4r_W^2 \gamma_W^2} \int_{-1}^{+1} dx \frac{1}{\left(\frac{(1-r^2)(x-1)-2r_W^2}{2r_W \gamma_W} \right)^2 + 1} \\
I_3 &= K \frac{1}{4r_W^2 \gamma_W^2} \frac{2r_W \gamma_W}{1-r^2} \int_{-\frac{(1-r^2)+r_W^2}{r_W \gamma_W}}^{-\frac{r_W}{\gamma_W}} du \frac{1}{u^2 + 1} \\
I_3 &= K \frac{1}{2r_W \gamma_W} \frac{1}{1-r^2} \left(\arctan \left(\frac{(1-r^2)+r_W^2}{r_W \gamma_W} \right) - \arctan \left(\frac{r_W}{\gamma_W} \right) \right)
\end{aligned}$$

Finally,

$$\begin{aligned}
\sigma_W &= \frac{g_W^4 V_{\ell k}^2}{128\pi s} \left[2(1-r^2) + (2-r^2+2r_W^2) \log \left(\frac{r_W^2(r_W^2 + \gamma_W^2)}{((1-r^2)+r_W^2)^2 + r_W^2 \gamma_W^2} \right) \right. \\
&\quad \left. + 2 \frac{-r^2(1+r_W^2) + (1+2r_W^2) + r_W^2(r_W^2 - \gamma_W^2)}{r_W \gamma_W} \left(\arctan \left(\frac{(1-r^2)+r_W^2}{r_W \gamma_W} \right) - \arctan \left(\frac{r_W}{\gamma_W} \right) \right) \right]
\end{aligned}$$

Process $e^+ e^- \longrightarrow h \longrightarrow \bar{\nu}_e N_1$

Calculation of the matrix element



Start by calculating $i\mathcal{M}$:

$$i\mathcal{M} = \left[\bar{v}_b \left(\frac{-ig_W m_e}{2m_W} \right) u_a \right] \left[\frac{-i}{q^2 - m_h^2 + im_h \Gamma_h} \right] \left[\bar{u}_1 \left(\frac{-ig_W m_1}{2m_W} V_{\ell k} P_R \right) v_2 \right]$$

$$i\mathcal{M} = \frac{ig_W^2 V_{\ell k} m_e m_1}{4m_W^2 (s - m_h^2 + im_h \Gamma_h)} \left[\bar{v}_b u_a \right] \left[\bar{u}_1 P_R v_2 \right]$$

Then we calculate $i\mathcal{M}^\dagger$:

$$-i\mathcal{M}^\dagger = \frac{-ig_W^2 V_{\ell k} m_e m_1}{4m_W^2 (s - m_h^2 - im_h \Gamma_h)} \left[\bar{v}_2 P_L u_1 \right] \left[\bar{u}_a v_b \right]$$

We can then calculate $|\mathcal{M}|^2$

$$|\mathcal{M}|^2 = \frac{g_W^4 V_{\ell k}^2 m_e^2 m_1^2}{16m_W^4 \left((s - m_h^2)^2 + (m_h \Gamma_h)^2 \right)} \left[\overline{v_b} u_a \right] \left[\overline{u_1} P_R v_2 \right] \left[\overline{v_2} P_L u_1 \right] \left[\overline{u_a} v_b \right]$$

We now calculate $|\overline{\mathcal{M}}|^2$:

$$\begin{aligned} |\overline{\mathcal{M}}|^2 &= \sum_{s_1, s_2} \times \frac{1}{2} \sum_{s_a} \times \frac{1}{2} \sum_{s_b} |\mathcal{M}|^2 \\ &= \frac{g_W^4 V_{\ell k}^2 m_e^2 m_1^2}{64m_W^4 \left((s - m_h^2)^2 + (m_h \Gamma_h)^2 \right)} \text{Tr}(\not{p}_a \not{p}_b) \text{Tr}(\not{p}_1 \not{p}_2 P_L) \\ &= \frac{g_W^4 V_{\ell k}^2 m_e^2 m_1^2}{8m_W^4 \left((s - m_h^2)^2 + (m_h \Gamma_h)^2 \right)} (p_a p_b) (p_1 p_2) \\ &= \frac{g_W^4 V_{\ell k}^2 m_e^2 m_1^2}{32m_W^4 \left((s - m_h^2)^2 + (m_h \Gamma_h)^2 \right)} (s^2 - s m_1^2) \end{aligned}$$

We can now compute the differential cross section :

$$\frac{d\sigma^*}{d\Omega^*} = \frac{1}{64\pi^2 s} \left(1 - \frac{m_1^2}{s} \right) |\overline{\mathcal{M}}|^2$$

We integrate to obtain the effective cross-section :

$$\begin{aligned} \sigma &= \int_{\phi=0}^{2\pi} \int_{\cos\theta=-1}^1 \frac{d\sigma^*}{d\Omega^*} d\cos\theta d\phi \\ &= 4\pi \times \frac{1}{64\pi^2 s} \left(1 - \frac{m_1^2}{s} \right) |\overline{\mathcal{M}}|^2 \\ &= \frac{g_W^4 V_{\ell k}^2 m_e^2}{512\pi m_W^4 \left((s - m_h^2)^2 + (m_h \Gamma_h)^2 \right)} \end{aligned}$$

In the end, we have :

$$\sigma = \frac{g_W^4 V_{\ell k}^2 m_e^2}{512\pi m_W^4 \left((s - m_h^2)^2 + (m_h \Gamma_h)^2 \right)} \frac{m_1^2}{s} \left(1 - \frac{m_1^2}{s} \right) (s^2 - s m_1^2)$$

Interference terms

$$|\mathcal{M}|^2 = |\mathcal{M}_Z|^2 + |\mathcal{M}_W|^2 + |\mathcal{M}_h|^2 - 2\text{Re} \left(\mathcal{M}_Z \mathcal{M}_W^\dagger \right) + 2\text{Re} \left(\mathcal{M}_Z \mathcal{M}_h^\dagger \right) - 2\text{Re} \left(\mathcal{M}_W \mathcal{M}_h^\dagger \right)$$

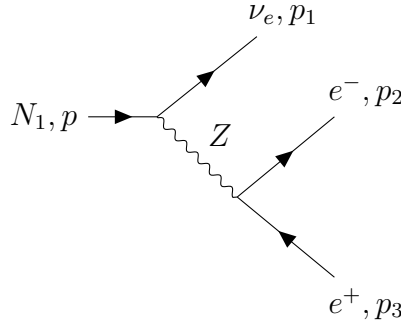
- $-2\text{Re} \left(\mathcal{M}_W \mathcal{M}_h^\dagger \right) = 0$

- $+2\text{Re} \left(\mathcal{M}_Z \mathcal{M}_h^\dagger \right) = 0$
- $-2\text{Re} \left(\mathcal{M}_Z \mathcal{M}_W^\dagger \right) = \frac{e^2 |V|^2 c_L^e g_W^2}{4c_W^2 s_W^2} \cdot \frac{(s - m_Z^2)(t - m_W^2) + m_W m_Z \Gamma_W \Gamma_Z}{[(s - m_Z^2)^2 + m_Z^2 \Gamma_Z^2] [(t - m_W^2)^2 + m_W^2 \Gamma_W^2]} \cdot (s + t)(m^2 - s - t)$

$$\sigma_{WZ} = \frac{g_Z^2 |V|^2 c_L^e g_W^2}{128 \pi s} \cdot \frac{\left(1 - \frac{m^2}{s}\right) (m^2 - s)}{(s - m_Z^2)^2 + m_Z^2 \Gamma_Z^2} \cdot \int_{-2}^0 dx \frac{\left(s - \frac{1}{2}x(m^2 - s)\right) \left(\frac{1}{2}x + 1\right) \left(\frac{1}{2}x(m^2 - s)(m_Z^2 - s) - sm_W^2 + m_W m_Z \Gamma_W \Gamma_Z + m_W^2 m_Z^2\right)}{\left(m_W^2 + \frac{1}{2}x(m^2 - s)\right)^2 + m_W^2 \Gamma_W^2}$$

Decay width of N_e

Calculation of the decay width



We get the same matrix element as the s-channel with Z boson :

$$|\overline{\mathcal{M}}|^2 = \frac{g_Z^4 (V_{lk})^2 (C_L^2 + C_R^2)}{2 \left(((p_2 + p_3)^2 - m_Z^2)^2 + (m_Z \Gamma_Z)^2 \right)} (p \cdot p_3)(p_1 \cdot p_2)$$

We can introduce the generalised Mandelstam variable :

$$\begin{aligned} m_{12}^2 &= (p_1 + p_2)^2 = (p - p_3)^2 \\ m_{13}^2 &= (p_1 + p_3)^2 = (p - p_2)^2 \\ m_{23}^2 &= (p_2 + p_3)^2 = (p - p_1)^2 \\ m_{12}^2 + m_{13}^2 + m_{23}^2 &= M^2 + m_1^2 + m_2^2 + m_3^2 \end{aligned}$$

In our case, we neglect the mass m_1 , m_2 and m_3 (M is the HNL mass) :

$$m_{12}^2 + m_{13}^2 + m_{23}^2 = M^2$$

We can express $(p \cdot p_3)(p_1 \cdot p_2)$ with those generalised Mandelstam variable

$$\begin{aligned} (p - p_3)^2 = M^2 - 2pp_3 &\implies p \cdot p_3 = \frac{M^2 - m_{12}^2}{2} \\ (p_1 + p_2)^2 = 2p_1 p_2 &\implies p_1 \cdot p_2 = \frac{m_{12}^2}{2} \end{aligned}$$

And we want to express by 2 of the 3 variables :

$$p \cdot p_3 = \frac{m_{13}^2 + m_{23}^2}{2}$$

$$p_1 \cdot p_2 = \frac{M^2 - m_{13}^2 - m_{23}^2}{2}$$

And the first mandelstam variable s change :

$$s - m_Z^2 = (p_2 + p_3)^2 - m_Z^2 = m_{23}^2 - m_Z^2$$

We can replace in the $|\overline{\mathcal{M}}|^2$ formula :

$$|\overline{\mathcal{M}}|^2 = \frac{g_Z^4 (V_{\ell k})^2 (C_L^2 + C_R^2)}{8 \left((m_{23}^2 - m_Z^2)^2 + (m_Z \Gamma_Z)^2 \right)} m_{12}^2 (M^2 - m_{12}^2)$$

The decay width formula for a three body decay is :

$$d\Gamma = \frac{1}{(2\pi)^3} \frac{1}{32M^3} |\overline{\mathcal{M}}|^2 dm_{12}^2 dm_{23}^2$$

Then to obtain the integrated decay width :

$$\Gamma = \int_{m_{12}^2=0}^{M^2} \int_{m_{23}^2=0}^{M^2 - m_{12}^2} d\Gamma$$

We integrate over m_{23}^2 :

$$\Gamma = \frac{g_Z^4 (V_{\ell k})^2 (C_L^2 + C_R^2)}{8 \cdot 32M^3 \cdot (2\pi)^3} \int_{x=0}^{M^2} x(M^2 - x) \int_{y=0}^{M^2 - x} \frac{1}{(y - m_Z^2)^2 + (m_Z \Gamma_Z)^2} dx dy$$

with:

$$\begin{aligned} & \int_{y=0}^{M^2 - x} \frac{1}{(y - m_Z^2)^2 + (m_Z \Gamma_Z)^2} dy \\ &= \frac{1}{m_Z \Gamma_Z} \left[\arctan \left(\frac{y - m_Z^2}{m_Z \Gamma_Z} \right) \right]_{y=0}^{M^2 - x} \\ &= \frac{1}{m_Z \Gamma_Z} \left(\arctan \left(\frac{M^2 - m_Z^2 - x}{m_Z \Gamma_Z} \right) + \arctan \left(\frac{m_Z}{\Gamma_Z} \right) \right) \end{aligned}$$

We integrate over m_{12}^2 :

$$\Gamma = \frac{g_Z^4 (V_{\ell k})^2 (C_L^2 + C_R^2)}{8 \cdot 32M^3 \cdot (2\pi)^3 \cdot m_Z \Gamma_Z} \int_{x=0}^{M^2} x(M^2 - x) \left(\arctan \left(\frac{M^2 - m_Z^2 - x}{m_Z \Gamma_Z} \right) + \arctan \left(\frac{m_Z}{\Gamma_Z} \right) \right) dx$$

We focus on the following integration I_1 :

$$I_1 = \int_{x=0}^{M^2} x(M^2 - x) \arctan \left(\frac{m_Z}{\Gamma_Z} \right) dx = \arctan \left(\frac{m_Z}{\Gamma_Z} \right) \left[-\frac{x^3}{3} + \frac{M^2 x^2}{2} \right]_{x=0}^{M^2}$$

$$= \arctan\left(\frac{m_Z}{\Gamma_Z}\right) \frac{M^6}{6}$$

We focus on the following integration I_2 :

$$\begin{aligned} I_2 &= \int_{x=0}^{M^2} x(M^2 - x) \arctan\left(\frac{M^2 - m_Z^2 - x}{m_Z \Gamma_Z}\right) dx \\ &= m_Z \Gamma_Z \int_{u=\frac{M^2 - m_Z^2}{m_Z \Gamma_Z}}^{-\frac{m_Z}{\Gamma_Z}} (M^2 - m_Z^2 - u m_Z \Gamma_Z) (m_Z^2 + u m_Z \Gamma_Z) \arctan u \, du \end{aligned}$$

Primitive identity:

$$\begin{aligned} &\int (ax^2 + bx + c) \arctan(x) \\ &= \frac{1}{6} [(2ax^3 + 3b(x^2 + 1) + 6cx) \arctan(x) + (a - 3c) \log(1 + x^2) - (ax^2 + 3bx)] \end{aligned}$$

Go back to I_2 :

$$\begin{aligned} I_2 &= [(-2(m_Z \Gamma_Z)^2 u^3 + 3m_Z \Gamma_Z (M^2 - 2m_Z^2)(u^2 + 1) + 6m_Z^2 (M^2 - m_Z^2)u) \arctan(u) \\ &+ m_Z^2 (-3M^2 + 3m_Z^2 - \Gamma_Z^2) \log(1 + u^2) + x m_Z \Gamma_Z (-m_Z \Gamma_Z x + 3(M^2 - 2m_Z^2))] \Big|_{u=\frac{M^2 - m_Z^2}{m_Z \Gamma_Z}}^{-\frac{m_Z}{\Gamma_Z}} \end{aligned}$$

$\beta\gamma$ and energy computation

We get with MadGraph the decay width Γ , so we can obtain the the proper lifetime :

$$\tau = \frac{\hbar}{\Gamma}$$

We create a neutrino (with neglected mass) and a HNL (with a mass m_1) so the conservation of energy is :

$$\sqrt{s} = E_N + E_\nu = \sqrt{p^2 + m_1^2} + p$$

so we can rewrite :

$$\begin{aligned} \sqrt{p^2 + m_1^2} - \sqrt{s} &= p \\ p^2 + m_1^2 + s - 2\sqrt{s}\sqrt{p^2 + m_1^2} &= p^2 \\ \sqrt{p^2 + m_1^2} &= \frac{s + m_1^2}{2\sqrt{s}} \\ p^2 &= \left(\frac{s + m_1^2}{2\sqrt{s}}\right)^2 - m_1^2 \\ p &= \frac{s - m_1^2}{2\sqrt{s}} \end{aligned}$$

And because $p = \beta\gamma m$:

$$\beta\gamma = \frac{p}{m} = \frac{s - m^2}{2m\sqrt{s}}$$

We also have :

$$E_N = \frac{s + m^2}{2\sqrt{s}}$$
$$E_\nu = \frac{s - m^2}{2\sqrt{s}}$$

Appendix E : Cards for generation and simulation

```
1 *****
2 **
3 **           W E L C O M E to
4 **       M A D G R A P H 5 _ a M C @ N L O
5 **           M A D E V E N T
6 **
7 **           *               *
8 **         *       * *       *
9 **       * * * * 5 * * * *
10 **        *       * *       *
11 **         *               *
12 **
13 **       VERSION 3.5.3               2023-12-23
14 **
15 **   The MadGraph5_aMC@NLO Development Team - Find us at
16 **   https://server06.fynu.ucl.ac.be/projects/madgraph
17 **
18 **           Type 'help' for in-line help.
19 **
20 # *****
21 # *
22 # Command File for MadGraph5_aMC@NLO *
23 # *
24 # run as ./bin/mg5_aMC filename *
25 # *
26 # *****
27 set default_unset_couplings 99
28 set group_subprocesses Auto
29 set ignore_six_quark_processes False
30 set loop_optimized_output True
31 set loop_color_flows False
32 set gauge unitary
33 set complex_mass_scheme False
34 set max_npoint_for_channel 0
35 set auto_convert_model T
36 import model sm
37 define p = g u c d s u~ c~ d~ s~
38 define j = g u c d s u~ c~ d~ s~
39 define l+ = e+ mu+
40 define l- = e- mu-
41 define vl = ve vm vt
42 define vl~ = ve~ vm~ vt~
43 # Here is the file of the model used
44 import model SM_HeavyN_CKM_AllMasses_LO
```

```

45 define e = e+ e-
46 define nue = ve ve~
47 generate e+ e- > z > ve~ n1
48 output e+e-_z_ven1
49 launch e+e-_z_ven1
50 done
51 # set to electron beams (0 for ele , 1 for proton)
52 set lpp1 0
53 set lpp2 0
54 # I take sqrt ( s ) = 91.188 GeV to be at the Z mass
55 set ebeam1 45.594
56 set ebeam2 45.594
57 set no_parton_cut
58 # Here I set mass of the electron HNL , from 0 to 90 GeV
59 set mn1 scan:[0,5,10,15,20,25,30,35,40,45,50,55,60,65,70,75,80,85,90]
60 # set mass of muon HNL , made heavy here
61 set mn2 10000
62 # set mass of tau HNL , made heavy here
63 set mn3 10000
64 # set electron mixing angle
65 set ven1 1
66 done

```

Example of a MadGraph script

```

1 Main:numberOfEvents = 200           ! number of events to generate
2 Main:timesAllowErrors = 3           ! abort run after this many flawed
   events
3 Init:showChangedSettings = on       ! list changed settings
4 Init:showAllSettings = off          ! list all settings
5 Init:showChangedParticleData = on   ! list changed particle data
6 Init:showAllParticleData = off      ! list all particle data
7 Next:numberCount = 1000             ! print message every n events
8 Next:numberShowLHA = 1              ! print LHA information n times
9 Next:numberShowInfo = 1             ! print event information n times
10 Next:numberShowProcess = 1          ! print process record n times
11 Next:numberShowEvent = 1           ! print event record n times
12
13 #Read everything from LHE file
14 Beams:frameType = 4
15 Beams:LHEF = unweighted_events.lhe.changed
16
17 #MasterSwitch Pythia
18 PartonLevel:MPI = on
19 PartonLevel:ISR = on
20 PartonLevel:FSR = on
21 PartonLevel:Remnants = on
22 HadronLevel:Hadronize = on
23 HadronLevel:Decay = on
24
25 #No limit for flying particles
26 ParticleDecays:limitTau0 = off
27 ParticleDecays:tau0Max = 100000
28 ParticleDecays:tauMax = 100000

```

Example of a Pythia script